Title: Erythropoietin directly remodels the clonal composition of murine hematopoietic multipotent progenitor cells

A.S. Eisele[1], J. Cosgrove[1], A. Magniez[1], E. Tubeuf[1], S. Tenreira Bento[1], C. Conrad[1], F. Cayrac[1], T. Tak[1], A.M. Lyne[1], J. Urbanus[2] and L. Perié[1*].

Affiliations

1. Institut Curie, Université PSL, Sorbonne Université, CNRS UMR168, Laboratoire Physico Chimie Curie, 75005 Paris, France
2. Netherlands Cancer Institute, Amsterdam, Netherlands

Contact information

Leila Perié, Postal address: UMR168, Institute Curie, 11 rue Pierre et Marie Curie, 75005 Paris, Leila.Perie@curie.fr, +33156246229.

Abstract

The cytokine erythropoietin (EPO) is a potent inducer of erythrocyte development and one of the most prescribed biopharmaceuticals. The action of EPO on erythroid progenitor cells is well established, but its direct action on hematopoietic stem and progenitor cells (HSPCs) is still debated. Here, using cellular barcoding, we traced the differentiation of hundreds of single murine HSPCs, after *ex vivo* EPO-exposure and transplantation, in five different hematopoietic cell lineages, and observed the transient occurrence of high-output Myeloid-Erythroid-megaKaryocyte (MEK)-biased and Myeloid-B-cell-Dendritic cell (MBDC)-biased clones. Single-cell RNA sequencing (ScRNAseq) analysis of *ex vivo* EPO-exposed HSPCs revealed that EPO induced the upregulation of erythroid associated genes in a subset of HSPCs, overlapping with multipotent progenitor (MPP) 1 and MPP2. Transplantation of Barcoded EPO-exposed-MPP2 confirmed their enrichment in Myeloid-Erythroid-biased clones. Collectively, our data show that EPO does act directly on MPP independent of the niche, and modulates fate by remodeling the clonal composition of the MPP pool.

Introduction

Erythrocytes are the most numerous hematopoietic cells in our body and are constantly renewed[1]. The major inducer of erythroid cell development in steady state and anemic conditions is the cytokine EPO[2]. Recombinant EPO is widely used to treat anemia and is one of the most sold biopharmaceuticals[3]. Previously, EPO was thought to solely target erythroid-committed progenitors and induce their increased proliferation and survival via the EPO receptor (EPOR)[4]. Recently, EPO has also been suggested to act on HSPCs [5–12], but the nature of EPO´s effect on HSPC fate remains unresolved

50 despite potential adverse side effects during long-term EPO usage in the clinics and
51 associations of high EPO levels with leukemias[13–15].
52 It is well established that EPO can induce HSPCs to cycle, as evidenced by a number
53 of bulk and single cell studies *in vitro* and *in vivo*[5,12,8,9,11]. It's role in modulating HSPC
54 fate is less clear however, with a lack of studies that functionally assess HSPC fate at
55 the single cell level *in vivo*, and analyze the direct effect of EPO on HSPCs, and not
56 the effect of the surrounding niche. More specifically, the upregulation of erythroid
57 associated genes in HSPC (LSK CD150$^+$ Flt3$^-$ CD48$^-$) in response to *in vivo* EPO has
58 been observed with bulk transcriptomics[11], suggesting that HSPCs deviate their fate
59 toward erythroid production. Recent ScRNAseq analysis observed different changes
60 of lineage-associated gene expressions after *in vivo* EPO-exposure of HSPCs[9,8]. As
61 changes of gene expression do not necessarily result in cell fate modification[14],
62 functional validations *in vivo* are necessary. In one study such functional validation was
63 performed using bulk transplantation of *in vivo* EPO-exposed HSPCs (LSK CD150$^+$
64 Flt3$^-$)[7]. This study showed increased erythroid production and decreased myeloid cell
65 production, concluding that EPO deviates the fate of HSPCs in favor of erythroid
66 production. As EPO has also been shown to target hematopoietic niche cells
67 (osteoblasts and osteocytes[15,16] endothelial cells[17,16], adipocytes[18,19], and
68 mesenchymal stem cells[6,20]), it remains however still unclear whether EPO acts directly
69 on HSPCs, via their environment, or both.
70 It is now established that HSPCs encompass cells with different long-term
71 reconstitution capacity after transplantation, as well as a heterogeneous output in
72 terms of quantity (lineage-bias) and type of cells (lineage-restriction)[21–28]. Recently, the
73 HSPC compartment was subdivided into long-term hematopoietic stem cells (LT-HSC)
74 and different multipotent progenitors (MPP) (MPP1-4[29,30]), with variation around the

75 phenotypic definition[31]. Interestingly, HSPC composition responds to irradiation with
76 HSC transiently self-renewing less and increasing their production of MPP2-3[31]. In the
77 case of EPO, conflicting results suggest that either HSC or MPP respond to EPO [8,9,11]
78 but the difference in HSPC definition and the lack of functional validation make it
79 difficult to compare these studies. As HSPCs are functionally heterogeneous, and the
80 current phenotypic definition partially capture this heterogeneity, a single cell in vivo
81 lineage tracing approach is needed to assess whether EPO can influence HSPC fate
82 decisions.
83 To analyze the functional effect of EPO on the differentiation of individual HSPCs (C-
84 Kit$^+$ Sca1$^+$ CD150$^+$ Flt3$^-$) removing the effect of the niche, we here utilized cellular
85 barcoding technology which allowed us to trace the progeny of hundreds of single
86 HSPCs *in vivo*. By analyzing cellular barcodes in five mature hematopoietic lineages
87 and HSPCs, we observed transient induction of high-output MEK-biased barcode
88 clones compensated by MBDC-biased clones after ex vivo EPO-exposure. ScRNAseq
89 of *ex vivo* EPO-exposed HSPCs revealed upregulation of erythroid associated genes
90 in a subset of the compartment with overlap to gene signatures of MPP1 (C-Kit$^+$ Sca1$^+$
91 Flt3$^-$ CD150$^+$ CD48$^-$ CD34$^+$), and MPP2 (C-Kit$^+$ Sca1$^+$ Flt3$^-$ CD150$^+$ CD48$^+$)[30,29] and not
92 of LT-HSCs (C-Kit$^+$ Sca1$^+$ Flt3$^-$ CD150$^+$ CD48$^-$ CD34$^-$). Transplantation of barcoded
93 MPP2 confirmed their enrichment in ME-biased clones in response to EPO. Moreover,
94 the increased contribution of biased HSPC clones to the mature cell lineages after
95 EPO-exposure did not match their frequency in HSPCs, indicating that they were
96 differentiating more than self-renewing, a property associated to multipotent
97 progenitors. The transient effect of EPO on HSPCs further corroborates an action of
98 EPO on MPP1/2 rather than LT-HSCs. Altogether our results are consistent with a
99 model in which perturbations induce clonal remodeling of HSPC contributing to

100 hematopoiesis, with biased MPPs transiently contributing more than LT-HSC. They
101 also demonstrate a direct effect of EPO on MPPs after transplantation with implications
102 for basic HSC research and therapeutic applications in the clinic.
103
104 **Results**
105 **EPO-exposure induces biases in single HSPCs.** Given the debate surrounding
106 which HSPC subset is responding to EPO, we decided to analyzed the direct effect of
107 EPO on the differentiation of HSPCs defined as C-Kit$^+$ Sca1$^+$ Flt3$^-$ CD150$^+$
108 (encompassing LT-HSC (C-Kit$^+$ Sca1$^+$ Flt3$^-$ CD150$^+$ CD48$^-$ CD34$^-$), MPP1 (C-Kit$^+$
109 Sca1$^+$ Flt3$^-$ CD150$^+$ CD48$^-$ CD34$^+$), and MPP2 (C-Kit$^+$ Sca1$^+$ Flt3$^-$ CD150$^+$ CD48$^+$)[30,29])
110 at the single cell level by cellular barcoding. To this purpose, we generated a new high-
111 diversity lentiviral barcode library (LG2.2, 18,026 barcodes in reference list), consisting
112 of random 20 nucleotides sequences positioned adjacent to the green fluorescent
113 protein (GFP) gene, enabling the tracking of many individual cells in parallel. Using this
114 LG2.2 library, we labeled single HSPCs (Figure 1- figure supplement 1a) with unique
115 genetic barcodes as previously described[33], exposed them to EPO (1,000 ng/ml) or
116 PBS for 16 hours *ex vivo* and transplanted around 2,600 cells (Mean 2,684 cells +/-
117 175 cells) of which around 10% barcoded cells into irradiated mice (Figure 1a). Note
118 that HSPCs kept their sorting phenotype after *ex vivo* culture albeit a slight
119 downregulation of C-Kit[44] and Flt3 (Figure 1 – figure supplement 1f). At day 30 after
120 transplantation, the earliest timepoint at which HSPCs produce simultaneously
121 erythroid, myeloid and lymphoid cells[45], barcoded (GFP$^+$) erythroblasts (E; Ter119$^+$
122 CD44$^+$[34]), myeloid cells (M; Ter119$^-$ CD19$^-$ CD11c$^-$ CD11b$^+$), and B-cells (B; Ter119$^-$
123 CD19$^+$) (Figure 1 – figure supplement 1b-c, e) were sorted from the spleen and their
124 barcode identity assessed through PCR and deep-sequencing. Note that bone and

125 spleen had similar barcoding profiles (Figure 1 – figure supplement 2). No difference
126 in chimerism was observed between the EPO and control group in the spleen and
127 blood, even when mTdTomato/mGFP donor mice were used to better assess the
128 erythroid lineage (Figure 1b-c). On average, we detected around eighty barcodes per
129 mouse, of which most were detected in several lineages (Figure 1d). Comparison of
130 the numbers of barcodes producing each lineage showed that EPO-exposure resulted
131 in the same number of engrafting and differentiating cells as in control (Figure 1d).
132 Notably, the number of erythroid restricted cells remained stable in the EPO group as
133 compared to control (Figure 1e), indicating that the response to EPO is more complex
134 than a direct instruction of erythroid-restricted HSPCs.
135 To quantify the effect of EPO on HSPC lineage-biases, barcode-labeled HSPCs were
136 classified based on the balance of their cellular output in the M, B and E lineages. With
137 this classification using a 10% threshold, cells classify for example as ME-biased if
138 they have above 10% of their output in the M and E lineage, and under 10% of their
139 output in the B lineage (Figure 1e other thresholds in Figure 1 – figure supplement 3b).
140 Interestingly, application of this classification revealed that although the proportion of
141 lineage-biased HSPCs in control and EPO group was similar (Figure 1f), their
142 contribution to the different lineages was increased by EPO-exposure (Figure 1g). In
143 the control group, balanced HSPCs (MBE) produced the majority of all lineages, as
144 previously published[46]. In the EPO group, ME- and MB-biased clones produced most
145 cells of the analyzed lineages (Figure 1g). ME-biased HSPCs produced the majority of
146 erythroid cells (57% +/- 10%), MB-biased HSPCs produced the majority of B-cells
147 (58% +/- 36%), and ME- and MB-biased clones contributed the majority of myeloid
148 cells (MB-biased 45% +/- 38% and ME-biased 20% +/- 13%, together 65% +/- 25%).
149 To test the significance of this effect, we used a permutation test, which compares the

150 effect size between control and EPO group to the one of all random groupings of
151 mice[47]. The contributions of the ME- and of the MB-biased HSPC classes to the
152 different lineages were significantly different in EPO and control groups (Table 1).
153 These results were reproduced in an additional experiment (Figure 1 – figure
154 supplement 3c-f, Supplementary File 1). A lower EPO concentration (160 ng/ml) as
155 well as an additional single injection of EPO (133 ug/kg) during transplantation gave
156 similar results (Figure 2, Figure 2 – figure supplement 1a, Table 1). Also at six weeks
157 post transplantation, similar results were obtained (Figure 1 – figure supplement 4,
158 Supplementary File 1). In summary, *ex vivo* EPO priming of HSPCs modified the output
159 balance of HSPCs rather than the number of lineage-restricted and -biased cells.
160 Balanced clones produced a smaller percentage of the mature cells; ME-biased
161 HSPCs produced most of the erythroid cells and MB-biased HSPCs produced most of
162 the B cells.
163
164 **Contribution of ME- and MB-biased HSPCs to the DC and MkP lineage.** To further
165 characterize the cells produced by the ME-biased and MB-biased HSPCs, we repeated
166 our experimental setup including the analysis of the megakaryocyte and dendritic cell
167 (DC) lineages (Figure 3). Megakaryocyte Progenitors (MkP) were chosen as proxy for
168 the production of platelets which are not suitable for barcode analysis. Barcoded
169 (GFP^+) DCs (DC; Donor $Ter119^-$ $CD19^-$ $CD11c^+$ $CD11b^-$) and MkP (MkP; C-Kit^+ Sca-1^-
170 $CD150^+$ $CD41^+$) (Figure 1 – figure supplement 1c-e) were sorted together with M, E,
171 and B cells, 4 weeks after transplantation of control or EPO-exposed HSPCs (1,000
172 ng/ml). In both groups, the majority of clones produced also DCs (Figure 3a). In the
173 control group, balanced HSPCs produced the majority of DCs (65% +/- 9%) (Figure
174 3b). However, in the EPO group, balanced HSPCs decreased their contribution to the

175 DC lineage (36% +/-25%) and MB-biased HSPCs significantly increased their
176 contribution (86% +/- 43% EPO vs 22% +/- 11% control group) (Figure 3b, Table 1),
177 thus, they were MBDC-biased HSPCs. In contrast the ME-biased HSPCs produced
178 few DCs in both groups (Figure 3b), indicating that ME-biased HSPCs are restricted
179 both in their B and DC production compared to the M and E production.
180 The majority of the MkP production came from the ME-biased HSPCs in both groups
181 (58% +/- 21% control and 55% +/- 14% EPO group, Figure 3c-d), indicating that ME-
182 biased HSPCs were also MkP-biased HSPCs (thus MEK-biased). We did not detect a
183 high contribution of MkP-restricted HSPCs[25,24,48] to the MkP lineage (Figure 3d).
184 Finally, as high EPO-exposure has been linked to changes in macrophage numbers[49–
185 56] we analyzed the contribution of control and EPO-exposed HSPCs to the myeloid
186 lineage in more detail, but could not detect changes in the percentage of the different
187 myeloid subsets produced (Figure 3 – figure supplement 1a-c).
188
189 **Effect of EPO on short-term HSPC self-renewal**. In light of previous studies which
190 suggested changes in HSPC proliferation after *in vivo* EPO-exposure[5,12,8,9,11], we next
191 explored if the short-term self-renewal capacity of HSPCs was impacted. To this end,
192 we analyzed barcodes in bone marrow HSPCs in addition to the spleen E, M, and B
193 lineages at week 4 after transplantation of control or EPO-exposed HSPCs (160 and
194 1,000 ng/ml) (Figure 4). We reasoned that barcodes of HSPCs differentiating and
195 short-term self-renewing (dividing to give rise to other HSPCs) after transplantation are
196 detected in both compartments, while detection in only HSPCs or mature lineages
197 indicates a prevalence of short-term self-renewal or differentiation respectively. Most
198 of the barcodes detected in HSPCs overlapped with barcodes in the mature cells
199 (Figure 4b left) in both the control and two EPO groups, showing that most of the

200 transplanted cells had given rise to other HSPCs and differentiated irrespective of the
201 treatment. Some barcodes were only detected in mature cells (Figure 4b right),
202 indicating that some HSPCs had only differentiated or were below the limit of detection.
203 These HSPCs were equally abundant in the control and two EPO groups (Figure 4b
204 right).
205 To analyze if different lineage biases correlated to different short-term self-renewal
206 capacity, we analyzed the proportion of biased HSPC classes, as previously defined,
207 within the HSPC compartment (Figure 4c). In the control group, balanced and ME-
208 biased HSPCs contributed most to the HSPC reads (34% +/- 36% MBE and 37% +/-
209 34% ME-biased HSPCs), while barcodes of MB-biased HSPCs contributed less (15%
210 +/- 32%) (Figure 4c), a trend that has been previously described[57,58,25]. Surprisingly,
211 the pattern of contributions of different biased HSPC subsets to HSPC reads was
212 unchanged in the EPO groups (Figure 4c), implying that the extent of short-term self-
213 renewal was unchanged after *ex vivo* EPO-exposure.
214 To study if the increased production of cells by the ME- and MB-biased HSPCs to the
215 mature cells observed after *ex vivo* EPO-exposure (Figure 1-3) correlated with short-
216 term self-renewal capacity of HSPCs, we analyzed the contribution of barcodes
217 detected or not in HSPCs to the E, M, and B lineages (Figure 4d). In the control group,
218 the majority of mature cells were derived from barcodes also present in HSPCs.
219 However, in both EPO groups, the contribution of barcodes detected in HSPCs to
220 mature cells was significantly lower (Figure 4d, Table 1) implying that the increased
221 contribution of biased HSPC classes to the mature cell lineages after *ex vivo* EPO-
222 exposure was most likely caused by cells differentiating more than short-term self-
223 renewing.
224

225 **EPO-exposure induces an erythroid program in a subgroup of HSPCs.** To further
226 characterize the effect of EPO-exposure on HSPCs, we performed scRNAseq of
227 barcoded C-Kit$^+$ Sca1$^+$ Flt3$^-$ CD150$^+$ cells after *ex vivo* culture in medium supplemented
228 with EPO or PBS using the 10X Genomics Chromium platform. 1,706 cells from control
229 and 1,595 cells from the EPO group passed our quality control. To compare the HSPCs
230 injected with non-cultured hematopoietic cells, we generated a reference map of
231 44,802 C-kit$^+$ cells from[42] and used published signatures as detailed in the
232 supplementary materials and methods[31,43] to annotate this map (Figure 5 – figure
233 supplement 1a,b and e,f). Projection of our single cell data on this map showed that
234 both the control and the EPO-exposed HSPCs similarly overlapped with non-MPP4
235 LSK cells, according to their sorting phenotype (Figure 5 – figure supplement 1e,f).
236 These results indicate that neither the *ex vivo* culture itself nor the EPO treatment
237 dramatically affected the global identity of the sorted HSPCs.
238 When comparing the EPO and control group, we found 1,176 differentially expressed
239 genes (Figure 5a and Supplementary File 2) and this number was significantly higher
240 than the number expected due to chance (p-value=0,01) as assessed by permutation
241 testing. Among the most upregulated genes in the EPO-exposed HSPCs, were genes
242 with erythroid association as *Hbb-bs*, *Erdr1*, *Wtap*, *Kmt2d*, or *Nfia*[59], and GATA1
243 targets (*Abhd2*, *Cbx3*, *Kdelr2*, *Pfas*), cell cycle related genes (*Tubb5*, *Hist1h2ap*) as
244 well as genes previously described to be induced in HSPCs after *in vivo* EPO-
245 exposure, such as *Bmp2k*[6] and *Ifitm1*[8] (Figure 5a). Genes involved in stem cell
246 maintenance, such as *Serpina3g*, *Mecom, Txnip*, *Meis1*, *Pdzk1ip1*[8], *Sqstm1*[60],
247 *Smad7*[61], *Aes*[62], were among the most downregulated genes in the EPO-exposed
248 HSPCs (Figure 5a).

249 As our cellular barcoding data suggests that single HSPCs differ in their response to
250 EPO, we assessed the heterogeneity of EPO responses at the transcriptomic level.
251 UMAP-based visualization of the data suggested that a subgroup of EPO-exposed
252 cells was transcriptomically distinct (Figure 5b), independently of the number of PCA
253 components and genes used in the analysis (Figure 5 – figure supplement 1c). To test
254 this observation, we defined an EPO response signature based on differentially
255 expressed genes between the EPO and control group. Plotting the expression of the
256 EPO response signature at the single cell level showed that the majority of the
257 transcriptomic differences between the control and EPO group were indeed driven by
258 this small subgroup of cells (Figure 5c). Reasoning that this subgroup contains the
259 cells directly responding to EPO, we defined as EPO-responders, cells in the 90th
260 percentile of EPO response signature expression (Figure 5c) for subsequent analysis.
261 Importantly, unsupervised clustering analysis of the data (Figure 5 – figure supplement
262 2a-b) showed similar results. The genes encoding EPOR, as well as the alternative
263 EPO receptors EphB4, CD131, CRFL3 were equally expressed between the EPO-
264 responders, non-responders and control groups (Figure 5 – figure supplement 1d).
265 Reasoning that the EPO-responders correspond to MEK-biased HSPCs, we also
266 looked for potential MBDC-biased HSPCs but could not detect a subgroup of cells with
267 upregulation of lymphoid associated genes, suggesting that the MBDC-bias is not a
268 direct effect of EPO-exposure but more an indirect effect. In summary, the scRNAseq
269 analysis corroborated our functional barcoding data, showing that a subset of HSPCs
270 can respond directly to EPO stimulation.
271
272 **EPO-responder HSPCs overlap with MPP1 and MPP2 signatures.** As our barcode
273 analysis suggested that the effect of direct EPO-exposure on HSPCs is caused by cells

274 differentiating more than self-renewing, we next wanted to assess which of the HSPC
275 subsets are the EPO responders in our scRNAseq dataset. We annotated the UMAP-
276 based visualization of our data with published signatures of the HSC (dormant HSCs[40]
277 and LT-HSC[41]), MPP1[40] and MPP2[31] subsets included in our HSPC gate, and
278 analyzed its overlap with the previously defined EPO-responder and non-responder
279 cells (Figure 6a,b). Relative to the control group and non-responders of the EPO-
280 group, the EPO-responders had a reduced expression of HSC gene signatures and
281 increased expression of MPP1 and MPP2 signatures (Figure 6a,b). An annotation of
282 the reference map generated from data of[42] likewise showed a low overlap of EPO-
283 responders with the most quiescent HSC subsets (Figure 6c,d). The independent
284 analysis using unsupervised clustering further supported this result (figure 5 – figure
285 supplement 2c,d). All in all, our scRNAseq analysis implied that, in line with our
286 barcoding results, the HSPCs directly reacting to EPO are most likely multipotent
287 progenitor cells of the MPP1 and MPP2 subsets.
288
289 **EPO-exposure induces ME-biases in single MPP2.**
290 To confirm that MPP2 are a subset within HSPCs reacting directly to EPO as predicted
291 by the scRNAseq analysis, we transplanted barcoded control or EPO-exposed (1,000
292 ng/ml) MPP2 together with unbarcoded CD48$^-$ HSPCS (C-Kit$^+$ Sca1$^+$ Flt3$^-$ CD150$^+$
293 CD48$^-$), (Figure 7 – figure supplement 1a) and analyzed their barcoded progeny in the
294 E, M, and B lineages of the spleen at week 4 after transplantation (Figure 7). We found
295 an equivalent engraftment as for the entire HSPC compartment and no difference
296 between the EPO-treated and the control group (Figure 7a-b). Applying the same
297 classification as in Figure 1 to quantify the effect of EPO on MPP2 lineage-biases, we
298 observed that, as for the whole HSPC compartment, ME-biased cells contributed more

299 to the M and E lineages (Figure 7d-e, other threshold in Figure 7 – figure supplement
300 1c). Similarly to our data on whole HSPC compartment (Figure 1g) the proportion of
301 the differently biased-MPP2 was similar between control and EPO group (Figure 7c).
302 This data confirms that the MPP2 population is enriched in HSPCs responding to EPO.
303

304 **Transient effect of EPO-exposure.**

305 Finally, we reasoned that if EPO directly acts on multipotent progenitors MPP1/2 with
306 short reconstitution capacity after transplantation rather than long-term repopulating
307 HSC, then the EPO effect should be transient. To test this hypothesis, we repeated the
308 experiment and analyzed barcodes in the E, M, and B lineages at 4 months after
309 transplantation of control or EPO-exposed HSPCs (160 and 1,000 ng/ml) (Fig. 8). In
310 the control group, as reported before[63], the chimerism at 4 months was higher and the
311 number of barcodes detected was lower than at one month post-transplantation (Fig.
312 8c-d and 1b-d). We detected no significant changes in the clonal output of HSPCs
313 between control and EPO group at this timepoint (Fig. 8e), with the majority of cells in
314 all lineages produced by balanced HSPCs (Fig. 8a-b), implying that the effect of direct
315 EPO-exposure on HSPCs is transient. This confirms that the effect of direct EPO-
316 exposure on HSPCs is likely caused by multipotent progenitor cells with a short
317 reconstitution capacity after transplantation.
318

319 **Discussion**

320 EPO is a key regulator of hematopoiesis, and is classically considered to support the
321 proliferation and survival of erythroid committed progenitors. By analyzing the *in vivo*
322 fate of hundreds of EPO-stimulated vs untreated transplanted (c-Kit^{+} Sca1^{+} Flt3^{-}
323 CD150^{+}) HSPCs at the single-cell level, we established that EPO can change HSPC

324 differentiation in the absence of an EPO-stimulated bone marrow microenvironment.
325 Collectively our results yield 2 important conclusions: (i) EPO has a direct effect on
326 HSPCs, that is not solely due to the effects of EPO on the surrounding niche and (ii)
327 EPO directly remodels the clonal composition of HSPC by inducing fate biased MPP
328 and reducing the output of HSC.
329
330 Specifically, we observe that EPO induced MEK-biased (ME) and MBDC-biased (MB)
331 HSPCs that produced the majority (>60%) of mature hematopoietic cells at four and
332 six weeks after transplantation. In contrast, balanced HSPCs (MBE) had a reduced
333 output of mature cells in response to EPO. The increased erythroid-associated gene
334 signature in a subset of HSPCs after *ex vivo* EPO-exposure suggests that EPO directly
335 induces high output MEK-biased HSPCs, which is indirectly compensated for by the
336 occurrence of high-output of MBDC-biased HSPCs to maintain a balanced production
337 of hematopoietic cells.
338 These biased clones had a higher propensity to differentiate than to self-renew, and
339 their response to EPO was transient, suggesting that EPO-responsive cells are multi-
340 potent progenitors, and not LT-HSCs. This is supported by transcriptomic analysis
341 showing that EPO-responders express the MPP1/MPP2 gene-signatures.
342 Transplantation of barcoded EPO-exposed MPP2 confirmed their enrichment in ME-
343 biased clones in response to EPO.
344 Similar to studies that assessed the effect of high systemic EPO-exposure [10,9,11,8], we
345 found that multipotent progenitors, not HSC, are responding to EPO. The occurrence
346 of myeloid, megakaryocytic and erythroid gene expression in MPP1 after bleeding [9] is
347 in line with our findings. Previously, long-term EPO exposure in Tg6 transgenic mice
348 did however not change the in vitro differentiation outcome of MPP2 [11]. Furthermore,

349 we did not detect a fate deviation toward erythroid production at the expense of myeloid
350 production as seen for in vivo EPO-exposed HSPCs after transplantation[7]. These
351 differences could be due both to the duration and route of EPO exposure as well as
352 the indirect effects of systemic EPO-exposure through other cells, for example from
353 the bone marrow niche.
354 In addition, our data shows that direct cytokine-stimulation leads to a clonal remodeling
355 of the HSPC compartment, with a transient increase in the contribution of fate-biased
356 MPPs. Without longitudinal barcoding data within the same animal, we cannot
357 distinguish if EPO is transiently changing the fate and outcome of the same HSPCs
358 over time or if EPO is pushing the differentiation of some HSPCs that will be replaced
359 by more balanced and stable HSPCs.
360 Different studies have suggested that the behavior of transplanted HSPC differ from
361 native HSPC[64,65]. Transplantation seems to favor the long-term output from HSC
362 whereas steady state hematopoiesis is maintained more by MPPs contribute than LT-
363 HSC[64,65,66]. Our work is in line with a model in which MPP are a highly malleable cell
364 population that can rapidly respond to changing demands for new cells, such as
365 transplantation or infection[31].
366 The direct effect of EPO on MPPs we described here could be one of the factors
367 underlying the development of adverse side effects and co-morbidities during long-
368 term EPO use in the clinics and associations of high EPO levels with leukemias[67,13,68].
369 To translate these results to the clinics and understand the side effect of EPO
370 treatment, further work is required to determine if HSPCs and erythroid progenitors like
371 CFU-E are responding to the same dose and duration of EPO exposure.

372 **Materials and Methods**

Key Resources Table

Reagent type (species) or resource	Designation	Source or reference	Identifiers	Additional information
Strain, strain background (*Mus musculus*)	C57BL/6J CD45.1^{+},	Jackson Laboratory	B6.SJL-*Ptprc*^{a} *Pepc*^{b}/BoyJ, stock No 002014, B6 Cd45.1	male
Strain, strain background(*Mus musculus*)	C57BL/6J CD45.2^{+},	Jackson Laboratory	C57BL/6J, stock No 000664, B6	male
Strain, strain background (*Mus musculus*)	*Rosa26CreER*^{T2};*mT/mG*	Jackson Laboratory	STOCK *Gt(ROSA)26Sor*$^{tm4(ACTB-tdTomato,-EGFP)Luo}$/J, stock No 007576, mT/mG, mTmG	male
Strain, strain background (*Escherichia coli*)	ElectroMAX™ Stbl4™ Competent Cells	ThermoFisher Scientific	Cat# 11635018	
Recombinant DNA reagent	pRRL-CMV-GFP plasmid[32]	PMID 9765382		Ton Schumacher lab, NKI, Amsterdam
Cell line (*human*)	HEK293T cells	other		Philippe Benaroch lab, Institute Curie, Paris
Recombinant DNA reagent	p8.9-QV	other		Philippe Benaroch lab, Institute Curie, Paris
Recombinant DNA reagent	pVSVG	other		Philippe Benaroch lab, Institute Curie, Paris

Chemical compound, drug	anti-CD117 magnetic beads	Miltenyi	Cat# 130-091-224, **RRID:AB_2753213**	
Chemical compound, drug	Propidium iodide	Sigma	Cat# 81845	
Chemical compound, drug	StemSpanMedium SFEM	STEMCELL Technologies	Cat# 9650	
Chemical compound, drug	Mouse recombinant SCF	STEMCELL Technologies	Cat# 78064.2	
Chemical compound, drug	Eprex, erythropoietin alpha	Janssen		
Chemical compound, drug	anti-biotinylated beads	Miltenyi	Cat# 130090485, **RRID:AB_244365**	
Antibody (rat, monoclonal)	anti-Ter119-biotin	BD Biosciences	Cat# 553672, clone TER119, **RRID:AB_394985**	(1:100)
Antibody (mouse, monoclonal)	anti-cd45.1-PE	BD Biosciences	Cat# 553776, clone A20, **RRID:AB_395044**	(1:100)
Antibody (rat, monoclonal)	anti-Ter119-PE-Cy7	BD Biosciences	Cat# 557853, clone TER119, **RRID:AB_396898**	(1:100)
Antibody (hamster, monoclonal)	anti-cd11c-APC	eBioscience	Cat# 17-0114-82, clone N418, **RRID:AB_469346**	(1:100)
Antibody (rat, monoclonal)	anti-cd19-APC-Cy7	BD Biosciences	Cat# 557655, clone ID3, **RRID:AB_396770**	(1:100)

Antibody (rat, monoclonal)	anti-cd11b-PerCP-Cy5.5	eBioscience s	Cat# 45-0112-82, clone M1/70, **RRID:AB_953 558**	(1:100)
Antibody (rat, monoclonal)	anti-cd117-APC	BioLegend	Cat# 105812, clone 2B8, **RRID:AB_313 221**	(1:100)
Antibody (rat, monoclonal)	anti-cd135-PE	eBioscience s	Cat# 12 135182, clone A2F10, **RRID:AB_465 859**	(100)
Antibody (rat, monoclonal)	anti-cd135-PE-Cy5	Life technologie s	Cat# 15_1351_82, clone A2F10, **RRID:AB_494 219**	(1:100)
Antibody (rat, monoclonal)	anti-Sca1-PacificBlue	BioLegend	Cat# 122520, clone D7, **RRID:AB_214 3237**	(1:200)
Antibody (rat, monoclonal)	anti-cd150-PE-Cy7 (Mouse-monoclonal)	BioLegend	Cat# 115914, clone TC15-12F12.2, **RRID:AB_439 797**	(1:100)
Antibody (rat, monoclonal)	anti-cd44-PE	BD Biosciences	Cat# 553134, clone IM7, **RRID:AB_394 649**	(100)
Antibody (rat, monoclonal)	anti-cd41-BV510	BD Biosciences	Cat# 740136, clone MVVREG30, **RRID:AB_273 9892**	(1:100)
Antibody (rat, monoclonal)	anti-Siglec-F-PE-CF594	BD Biosciences	Cat# 562757, clone E50-2440, **RRID:AB_268 7994**	(1:200)
Antibody (rat, monoclonal)	anti-Ly6g-BV510	BioLegend	Cat# 127633. clone 1A8, **RRID:AB_256 2937**	(1:200)

Antibody (rat, monoclonal)	anti-cd115-PE	BioLegend	Cat# 135505, clone AFS98, **RRID:AB_1937254**	(1:200)
Antibody (hamster, monoclonal)	anti-cd48-APC-Cy7	BD Biosciences	Cat# 561242 clone HM48-1, **RRID:AB_10644381**	(1:100)
Chemical compound, drug	Viagen Direct PCR Lysis Reagent (cell)	Euromedex	Cat# 301-C	
Chemical compound, drug	Proteinase K Solution RNA grade	Invitrogen	Cat# 25530-049	
Sequence-based reagent	top-LIB	This paper	PCR primer	TGCTGCCG TCAACTAG A ACA
Sequence-based reagent	bot-LIB	This paper	PCR primer	GATCTCGA ATCAGGCG CTTA
Sequence-based reagent	PCR2-Read1-plate-index-forward	This paper	PCR primer	ACACTCTTT CCCTACAC GACGCTCT TCCGATCT NNNNCTAG AACACTCG AGATCAG
Sequence-based reagent	PCR2-Read2-reverse	This paper	PCR primer	GTGACTGG AGTTCAGA CGTGTGCT CTTCCGAT CGATCTCG AATCAGGC GCTTA
Sequence-based reagent	PCR3-P5-forward	This paper	PCR primer	AATGATA CGGCGACC ACCGAGAT CTACACTC TTTCCCTA CACGACGC TCTTCCGA TCT
Sequence-based reagent	PCR3-P7-sample-index-reverse	This paper	PCR primer	CAAGCAGA AGACGGCA TACGAGAN NNNNNNGT

				GACTGGAG TTCAGA CGTGCTCT TCCGATC
Commercial assay or kit	Agencourt AMPure XP system	Beckman Coulter	Cat# A63881	
Commercial assay or kit	Chromium Single Cell 3' Reagent Kits v2 Chemistry	10X Genomics		
Software, algorithm	R-3.4.0	other		(R Development Core Team (2019) http://www.R-project.org
Software, algorithm	GraphPad Prism version 8.0 for Mac	GraphPad	**RRID:SCR_002798**	GraphPad Software, La Jolla California USA, www.graphpad.com
Software, algorithm	XCALIBR	other		(https://github.com/NKI-GCF/xcalibr)
Software, algorithm	Cellranger v3	10X Genomics	**RRID:SCR_017344**	
Software, algorithm	Seurat v3	DOI 10.1016/j.cell.2019.05.031	**RRID:SCR_007322**	

373

374 **Mice**

375 Male C57BL/6J CD45.1^{+}, C57BL/6J CD45.2^{+}, and *Rosa26CreER*^{T2};*mT/mG* mice from
376 Jackson Laboratory or bred at Institute Curie aged between 7-13 weeks were used in
377 all experiments. All procedures were approved by the responsible national ethics
378 committee (APAFIS#10955-201708171446318 v1).

379

380 **Barcode library, barcode reference list and lentivirus production**

381 The LG2.2 barcode library is composed of a DNA stretch of 180 bp with a 20 bp "N"-
382 stretch. DsDNA was generated by 10 PCR rounds and cloned into the XhoI-EcoRI site
383 of the lentiviral pRRL-CMV-GFP plasmid[32]. Subsequently ElectroMaxStbl4 cells were
384 transformed, and >10,000 colonies picked for amplification by Maxiprep. To create the
385 barcode reference list (https://github.com/PerieTeam/Eisele-et-al.-), barcode plasmids
386 were PCR amplified twice in duplicate and sequenced as described below. Sequencing
387 results were filtered for barcode reference list generation as previously described in[33].
388 Lentiviruses were produced by transfecting the barcode plasmids and p8.9-QV and
389 pVSVG into HEK293T cells in DMEM-Glutamax (Gibco) supplemented with 10% FCS
390 (Eurobio), 1% MEM NEAA (Sigma), and 1% sodium pyruvate (Gibco) using
391 Polyethyleneimine (Polysciences). Supernatant was 0,45 um filtered, concentrated by
392 1,5 h ultracentrifugation at 31,000g and frozen at -80°C. HEK293T were tested for
393 mycoplasma contamination every 6 months.

394

395 **HSPC and MPP2 isolation, barcoding, EPO treatment, and transplantation**

396 Isolation and labeling of cells with the barcoding library was performed as described
397 in[33]. Briefly, after isofluorane aneasthesia and cervical dislocation, bone marrow cells
398 were isolated from femur, tibia and iliac bones of mice by flushing, and C-Kit^{+} cells
399 were enriched with anti-CD117 magnetic beads on the MACS column system
400 (Miltenyi). Cells were stained for C-Kit, Flt3, CD150, Sca-1 (Key Resources Table)
401 Propidium iodide (PI) (Sigma) (1:5,000), and if appropriate CD48. Lineage staining was
402 not performed after C-Kit+ MACS enrichment for transplantation cohorts. For HSPC
403 cohorts, HSPCs (Figure 1 – figure supplement 1a) were sorted and transduced with
404 the barcode library in StemSpanMedium SFEM (STEMCELL Technologies) with 50

405 ng/ml mSCF (STEMCELL Technologies) through 1,5 h of centrifugation at 300 g and
406 4,5 h incubation at 37°C to obtain 10% barcoded cells. After transduction, cells were
407 incubated with human recombinant EPO (Eprex, erythropoietin alpha, Janssen) at a
408 final concentration of 1,000 or 160 ng/ml or PBS for 16 h at 37°C. After the incubation,
409 the cells were transplanted by tail vein injection in recipient mice 6 Gy sub-lethally
410 irradiated 3 hours before on a CIXD irradiator. Mice were allocated to groups of 4-5
411 mice for each condition randomly without masking. When indicated, cells were injected
412 together with additional EPO (133 ug/kg). On average 2,600 cells (Mean 2,684 cells
413 +/- 175 cells) were injected in the tail vein of each mouse. For the MPP2 cohort, MPP2
414 and $CD48^-$ HSPCs (Figure 7 – figure supplement 1a) were sorted. Both populations
415 were cultured alike, but only MPP2 were transduced with the barcode library and
416 treated with 1,000 ng/ml recombinant EPO as described above. After the culture,
417 barcoded MPP2 and un-barcoded $CD48^-$ HSPCs were mixed at a ratio of 32/45 (to be
418 as close as possible to the original ratio of both populations in the HSPCs) and
419 transplanted as described above. A FACSAria™ (BD Biosciences) was used for
420 sorting. FACSDiva™ software (BD Biosciences) was used for measurements and
421 FlowJo™ v.10 (TreeStar) for analysis.

422 **Cell progeny isolation for barcode analysis**

423 Spleens were mashed and both blood and spleen cells were separated based on
424 Ter119 using a biotinylated anti-Ter119 antibody (Key Resources Table) and anti-
425 biotinylated beads on the MACS column system (Miltenyi). $Ter119^+$ cells were stained
426 for Ter119 and CD44[34]. $Ter119^-$ cells were stained for CD45.1 CD11b, CD11c, CD19,
427 and if appropriate CD115, Siglec-F, and Ly6G (Key Resources Table). Bone marrow
428 cells were flushed from bones and enriched for C-Kit^+ cells as above. When
429 appropriate the C-Kit^- fraction was further separated based on Ter119 and stained as

430 above. C-Kit$^+$ cells were stained for C-Kit, Flt3, CD150, Sca-1, and if appropriate CD41
431 (Key Resources Table), and PI (1:5000) as described above. For analyzed and/or
432 sorted populations see Figure 1 – figure supplement 1. Populations were only sorted
433 for mice with an engraftment (donor cells percentage) of above 5% in spleen, bone
434 and blood.
435
436 **Lysis, barcode amplification and sequencing**
437 Sorted cells were lysed in 40 µl Viagen Direct PCR Lysis Reagent (cell) (Euromedex)
438 supplemented with 0,5 mg/ml Proteinase K Solution RNA grade (Invitrogen) at 55°C
439 for 120 min, 85°C for 30 min, 95°C for 5 min. Samples were then split into two
440 replicates, and a three-step nested PCR was performed to amplify barcodes and
441 prepare for sequencing. The first step amplifies barcodes (top-LIB
442 (5′TGCTGCCGTCAACTAGA ACA-3′) and bot-LIB (5′GATCTCGAATCAGGCGCTTA-
443 3′)). A second step adds unique 4 bp plate indices as well as Read 1 and 2 Illumina
444 sequences (PCR2-Read1-plate-index-forward
445 5'ACACTCTTTCCCTACACGACGCTCTTCCGATCTNNNNCTAGAACACTCGAGAT
446 CAG3′ and PCR2-Read2-reverse
447 5'GTGACTGGAGTTCAGACGTGTGCTCTTCCGAT
448 CGATCTCGAATCAGGCGCTTA3′). In a third step, P5 and P7 flow cell attachment
449 sequences and one of 96 sample indices of 7 bp are added (PCR3-P5-forward
450 5'AATGATA
451 CGGCGACCACCGAGATCTACACTCTTTCCCTACACGACGCTCTTCCGATCT3′
452 and PCR7-P7-sample-index-reverse
453 5'CAAGCAGAAGACGGCATACGAGANNNNNNNGTGACTGGAGTTCAGA
454 CGTGCTCTTCCGATC3′) (PCR program: hot start 5 min 95°C, 15 s at 95°C; 30 s at

455 57.2°C; 30 s at 72°C, 5 min 72°C, 30 (PCR1-2) or 15 cycles (PCR 3)). Both index
456 sequences (sample and plate) were designed based on[35] such that sequences differed
457 by at least 2 bp (https://github.com/PerieTeam/Eisele-et-al.-). To avoid lack of diversity
458 at the beginning of the reads, at least 4 different plate indices were used for each
459 sequencing run. Primers were ordered desalted, as high-performance liquid
460 chromatography (HPLC) purified. During lysis and each PCR, a mock control was
461 added. The DNA amplification by the three PCRs was monitored by the run on a large
462 2% Agarose gel. PCR3 products for each sample and replicate were pooled, purified
463 with the Agencourt AMPure XP system (Beckman Coulter), diluted to 5 nM. and
464 sequenced on a HiSeq system (Illumina) (SR-65bp) at Institute Curie facility with 10%
465 of PhiX spike-in.
466
467 **Barcode sequence analysis**
468 Sequencing results were filtered, and barcodes were categorized in progenitor classes
469 as in[33] and further explained on github (https://github.com/PerieTeam/Eisele-et-al.-).
470 In brief, sequencing results were analyzed using R-3.4.0 (R Development Core Team
471 (2019) http://www.R-project.org.), Excel, and GraphPad Prism version 8.0 for Mac
472 (GraphPad Software, La Jolla California USA, www.graphpad.com). Reads were first
473 filtered for perfect match to the input index- and common-sequences using XCALIBR
474 (https://github.com/NKI-GCF/xcalibr) and filtered against the barcode reference list.
475 Samples were then filtered for containing at least 5000 reads and normalized to 10^5
476 per sample. Samples with a Pearson correlation between duplicates below 0.9 were
477 discarded and barcodes present in one of the two replicates were set to zero. Samples
478 with under 10 barcodes were filtered out, unless indicated in the figure legend. The
479 mean of the replicates was used for further processing. When the mean percentage of

480 barcodes shared between different sequencing runs was higher than within the same
481 sequencing run for mice of a same transduction batch, reads below the read quartile
482 of the mean percentage of barcodes shared between mice of a same transduction
483 batch but sequenced on different sequencing runs were set to zero in order to equalize
484 the barcode sharing between mice transplanted from a same transduction batch in
485 different sequencing runs to the barcode sharing between mice within each
486 sequencing run. After filtering, read counts of each barcode in the different cell lineages
487 were normalized enabling categorization into classes of biased output toward the
488 analyzed lineages using a threshold of 10% of barcode reads (Other thresholds in
489 Figure 1 – figure supplement 3c and Figure 7 – figure supplement 1c). Statistics on
490 barcoding results were performed using a permutation test as in [36]. Significance of flow
491 cytometry results was assessed using Student's T test. Some mice were excluded from
492 the analysis due to death before readout, or due to a donor cell engraftment <5%, as
493 well as the filtering out of mice for which one or more cell subset samples did not pass
494 the barcode data filtering steps as detailed above.
495
496 **ScRNAseq and analysis**
497 ScRNAseq was performed using the 10X Genomics platform on one pool of HSPCs
498 isolated from 8 mice, barcoded and culture with or without EPO for 16h *in vitro* as
499 described above. Sequencing libraries were prepared using the Chromium Single Cell
500 3' v2 kit and sequenced on a HiSeq system (Illumina) at Institut Curie NGS facility.
501 Data was analyzed using Cellranger v3 (10X Genomics), Seurat v3[37] and customized
502 scripts. Raw sequencing reads were processed using Cellranger. To obtain a
503 reads/cell/gene count table, reads were mapped to the mouse GRCm38.84 reference
504 genome. scRNAseq analysis was performed using Seurat[37]. During filtering, Gm, Rik,

505 and Rp genes were discarded as non-informative genes. Cells with less than 1,000
506 genes per cell and with a high percentage of mitochondrial genes were removed from
507 downstream analyses. Following our filtering procedures, the average UMI count per
508 cell was 5157, with mitochondrial genes accounting for 5% of this. The average
509 number of genes detected per cell was 2337. Cell cycle annotation using the cyclone
510 method from the scran R package showed that 2938 cells were in G1 phase, 233 cells
511 were in G2M phase, and 127 cells were in S phase. No batch effect was detected
512 between the EPO and no-EPO group, therefore no batch correction was applied. Data
513 normalization was performed using the default Seurat approach and differentially
514 expressed genes were determined using a logistic regression in Seurat. Unsupervised
515 clustering was performed on the significant variable genes using the ten first principle
516 component analysis followed by the non-linear dimensionality reduction technique
517 UMAP[38] (Figure 5 – figure supplement 2). Unsupervised Louvain clustering of the data
518 was performed across a range of resolution parameters and the resolution value that
519 led to the most stable clustering profiles was chosen[39] (Figure 5 – figure supplement
520 2). Annotation of the clusters was obtained by mapping published signatures using the
521 *AddModuleScore* method of Seurat. The signatures are defined in the following
522 publications: dHSC, and MPP1 signatures were obtained from[40]. The MolO LT-HSC
523 signature was taken from[41] and the MPP2 and 4 signature was taken from[31]. An excel
524 file listing the genes in these signatures is available on github
525 (https://github.com/PerieTeam/Eisele-et-al.-). To identify EPO-responder cells in the
526 EPO group, differential expression analysis was performed between control and EPO
527 groups (Lists of DEGs are available at https://github.com/PerieTeam/Eisele-et-al.-).
528 Subsequently, genes that were differentially expressed (adjusted p-value< 0.05)
529 between EPO and control groups were transformed into an EPO response signature

530 which when overlaid onto the UMAP based visualization was enriched only in a subset
531 of the EPO group cells. Briefly this signature was obtained by taking the background
532 corrected mean expression values of both the up and downregulated genes per cell
533 as implemented in the *AddModuleScore* method of Seurat. Within each cell these two
534 signature scores were used to create a composite EPO response score by subtracting
535 the downregulated response from the upregulated response signature. Cells in the
536 upper 90th percentile with regards to the expression of the EPO response signature
537 were labelled EPO responders.
538 To perform supervised cell type annotation, a reference map was generated from a
539 published single cell sequencing dataset of 44,802 C-Kit^{+} cells from[42]. Preprocessing
540 was performed using a scanpy pipeline[43]. Data was then visualized using the non-
541 linear non-dimensionality reduction technique UMAP[38]. Annotation of the reference
542 map was obtained by overlaying published signatures as above using the
543 *AddModuleScore* method of Seurat and also known markers as *Flt3*, *slamf1*, and
544 *Gata1* (Figure 5 – figure supplement 1b). For the erythroid progenitors these markers
545 are *Gata1, Klf1, Epor, Gypa, Hba-a2, Hba-a1* (figure 5 – figure supplement 1a). Cells
546 were mapped onto the reference map using a k-nearest neighbors mapping approach.
547 Briefly, for each cell in the query dataset, the nearest neighbors in PCA space of the
548 reference dataset were determined using the nn2 function of the RANN package and
549 the mean UMAP 1 and 2 coordinates of the 10 nearest neighbors were taken as the
550 reference point for the new cell of interest. To benchmark our mapping approach, cells
551 from an independent dataset of erythroid progenitors [10] were used without additional
552 pre-processing (Figure 5 – figure supplement 1a).
553
554 **Data sharing statement**

555 Raw data are available at zenodo DOI 10.5281/zenodo.5645045**.** All codes to filter
556 and process raw data, as well as filtered data are available at
557 https://github.com/PerieTeam/Eisele-et-al.-. Contact author is leila.perie@curie.fr.
558

559 **Acknowledgements**

560 We thank Dr. T. Schumacher for discussion and lentiviral library production and Dr. K
561 Duffy for advices on permutation testing. We thank the Institute Curie flow cytometry,
562 next generation sequencing, and animal facility. We thank Fahima Di Federico from
563 the UMR168 BMBC facility for amplifying the barcode plasmid pool.
564

565 **Disclosure of Conflict of interest**

566 The authors declare no competing interests.
567

568 **References**
569

570 1. Sender R, Fuchs S, Milo R. Are We Really Vastly Outnumbered? Revisiting the
571 Ratio of Bacterial to Host Cells in Humans. *Cell*. 2016;164(3):337–40.
572 2. Richmond TD, Chohan M, Barber DL. Turning cells red: signal transduction
573 mediated by erythropoietin. *Trends Cell Biol.* 2005;15(3):146–155.
574 3. Walsh G. Biopharmaceutical benchmarks 2014. *Nat. Biotechnol.*
575 2014;32(10):992–1000.
576 4. Koury MJ. Tracking erythroid progenitor cells in times of need and times of
577 plenty. *Exp. Hematol.* 2016;44(8):653–63.
578 5. Cheshier SH, Prohaska SS, Weissman IL. The effect of bleeding on
579 hematopoietic stem cell cycling and self-renewal. *Stem Cells Dev.*
580 2007;16(5):707–17.
581 6. Shiozawa Y, Jung Y, Ziegler AM, et al. Erythropoietin Couples Hematopoiesis
582 with Bone Formation. *PLoS One*. 2010;5(5):e10853.
583 7. Grover A, Mancini E, Moore S, et al. Erythropoietin guides multipotent
584 hematopoietic progenitor cells toward an erythroid fate. *J. Exp. Med.*
585 2014;211(2):181–188.
586 8. Giladi A, Paul F, Herzog Y, et al. Single-cell characterization of haematopoietic
587 progenitors and their trajectories in homeostasis and perturbed
588 haematopoiesis. *Nat. Cell Biol.* 2018;1.
589 9. Yang J, Tanaka Y, Seay M, et al. Single cell transcriptomics reveals
590 unanticipated features of early hematopoietic precursors. *Nucleic Acids Res.*
591 2017;45(3):1281–1296.
592 10. Tusi BK, Wolock SL, Weinreb C, et al. Population snapshots predict early
593 haematopoietic and erythroid hierarchies. *Nature*. 2018;555(7694):54–60.

11. Singh RP, Grinenko T, Ramasz B, et al. Hematopoietic Stem Cells but Not Multipotent Progenitors Drive Erythropoiesis during Chronic Erythroid Stress in EPO Transgenic Mice. *Stem Cell Reports*. 2018;10(6):1908–1919.
12. Dubart A, Feger F, Lacout C, et al. Murine pluripotent hematopoietic progenitors constitutively expressing a normal erythropoietin receptor proliferate in response to erythropoietin without preferential erythroid cell differentiation. *Mol. Cell. Biol.* 1994;14(7):4834–42.
13. Ma W, Kantarjian H, Zhang K, et al. Significant association between polymorphism of the erythropoietin gene promoter and myelodysplastic syndrome. *BMC Med. Genet.* 2010;11(1):163.
14. Weinreb C, Rodriguez-Fraticelli A, Camargo FD, Klein AM. Lineage tracing on transcriptional landscapes links state to fate during differentiation. *Science*. 2020;
15. Li C, Shi C, Kim J, et al. Erythropoietin Promotes Bone Formation through EphrinB2/EphB4 Signaling. *J. Dent. Res.* 2015;94(3):455–463.
16. Singbrant S, Russell MR, Jovic T, et al. Erythropoietin couples erythropoiesis, B-lymphopoiesis, and bone homeostasis within the bone marrow microenvironment. *Blood*. 2011;117(21):.
17. Ito T, Hamazaki Y, Takaori-Kondo A, Minato N. Bone Marrow Endothelial Cells Induce Immature and Mature B Cell Egress in Response to Erythropoietin. *Cell Struct. Funct.* 2017;42(2):149–157.
18. American Society of Hematology S, Alvarez JC, Noguchi CT. Blood. American Society of Hematology; 2017.
19. Zhang Y, Wang L, Dey S, et al. Erythropoietin action in stress response, tissue maintenance and metabolism. *Int. J. Mol. Sci.* 2014;15(6):10296–333.
20. Tari K, Atashi A, Kaviani S, et al. Erythropoietin induces production of hepatocyte growth factor from bone marrow mesenchymal stem cells in vitro. *Biologicals*. 2017;45:15–19.
21. Dykstra B, Kent D, Bowie M, et al. Long-Term Propagation of Distinct Hematopoietic Differentiation Programs In Vivo. *Cell Stem Cell*. 2007;1(2):218–229.
22. Morita Y, Ema H, Nakauchi H. Heterogeneity and hierarchy within the most primitive hematopoietic stem cell compartment. *J. Exp. Med.* 2010;
23. Oguro H, Ding L, Morrison SJ. SLAM family markers resolve functionally distinct subpopulations of hematopoietic stem cells and multipotent progenitors. *Cell Stem Cell*. 2013;13(1):102–16.
24. Sanjuan-Pla A, Macaulay IC, Jensen CT, et al. Platelet-biased stem cells reside at the apex of the haematopoietic stem-cell hierarchy. *Nature*. 2013;502(7470):232–6.
25. Carrelha J, Meng Y, Kettyle LM, et al. Hierarchically related lineage-restricted fates of multipotent haematopoietic stem cells. *Nature*. 2018;554(7690):106–111.
26. Yamamoto R, Morita Y, Ooehara J, et al. Clonal analysis unveils self-renewing lineage-restricted progenitors generated directly from hematopoietic stem cells. *Cell*. 2013;154(5):1112–1126.
27. Lu R, Neff NF, Quake SR, Weissman IL. Tracking single hematopoietic stem cells in vivo using high-throughput sequencing in conjunction with viral genetic barcoding. *Nat. Biotechnol.* 2011;29(10):928–33.
28. Verovskaya E, Broekhuis MJC, Zwart E, et al. Heterogeneity of young and aged murine hematopoietic stem cells revealed by quantitative clonal analysis

644 using cellular barcoding. *Blood*. 2013;122(4):523–532.
645 29. Wilson A, Laurenti E, Oser G, et al. Hematopoietic Stem Cells Reversibly
646 Switch from Dormancy to Self-Renewal during Homeostasis and Repair. *Cell*.
647 2008;135(6):1118–1129.
648 30. Cabezas-Wallscheid N, Klimmeck D, Hansson J, et al. Identification of
649 regulatory networks in HSCs and their immediate progeny via integrated
650 proteome, transcriptome, and DNA methylome analysis. *Cell Stem Cell*.
651 2014;15(4):507–522.
652 31. Pietras EM, Reynaud D, Kang Y-A, et al. Functionally Distinct Subsets of
653 Lineage-Biased Multipotent Progenitors Control Blood Production in Normal
654 and Regenerative Conditions. *Cell Stem Cell*. 2015;17(1):35–46.
655 32. Dull T, Zufferey R, Kelly M, et al. A Third-Generation Lentivirus Vector with a
656 Conditional Packaging System. *J. Virol.* 1998;72(11):8463.
657 33. Naik SH, Perié L, Swart E, et al. Diverse and heritable lineage imprinting of
658 early haematopoietic progenitors. *Nature*. 2013;496(7444):229–232.
659 34. Chen K, Liu J, Heck S, et al. Resolving the distinct stages in erythroid
660 differentiation based on dynamic changes in membrane protein expression
661 during erythropoiesis. *Proc. Natl. Acad. Sci.* 2009;106(41):17413–17418.
662 35. Faircloth BC, Glenn TC. Not All Sequence Tags Are Created Equal: Designing
663 and Validating Sequence Identification Tags Robust to Indels. *PLoS One*.
664 2012;7(8):e42543.
665 36. Tak T, Prevedello G, Simon G, et al. Hspcs display within-family homogeneity
666 in differentiation and proliferation despite population heterogeneity. *Elife*.
667 2021;10:.
668 37. Satija R, Farrell JA, Gennert D, Schier AF, Regev A. Spatial reconstruction of
669 single-cell gene expression data. *Nat. Biotechnol.* 2015;33(5):495–502.
670 38. McInnes L, Healy J, Saul N, Großberger L. UMAP: Uniform Manifold
671 Approximation and Projection. *J. Open Source Softw.* 2018;
672 39. Blondel VD, Guillaume JL, Lambiotte R, Lefebvre E. Fast unfolding of
673 communities in large networks. *J. Stat. Mech. Theory Exp.* 2008;
674 40. Cabezas-Wallscheid N, Buettner F, Sommerkamp P, et al. Vitamin A-Retinoic
675 Acid Signaling Regulates Hematopoietic Stem Cell Dormancy. *Cell*. 2017;
676 41. Wilson NK, Kent DG, Buettner F, et al. Combined Single-Cell Functional and
677 Gene Expression Analysis Resolves Heterogeneity within Stem Cell
678 Populations. *Cell Stem Cell*. 2015;
679 42. Dahlin JS, Hamey FK, Pijuan-Sala B, et al. A single-cell hematopoietic
680 landscape resolves 8 lineage trajectories and defects in Kit mutant mice.
681 *Blood*. 2018;131(21):e1–e11.
682 43. Wolf FA, Hamey FK, Plass M, et al. PAGA: graph abstraction reconciles
683 clustering with trajectory inference through a topology preserving map of single
684 cells. *Genome Biol.* 2019;
685 44. Matsuoka Y, Sasaki Y, Nakatsuka R, et al. Low level of C-kit expression marks
686 deeply quiescent murine hematopoietic stem cells. *Stem Cells*.
687 2011;29(11):1783–1791.
688 45. Boyer SW, Rajendiran S, Beaudin AE, et al. Clonal and Quantitative In Vivo
689 Assessment of Hematopoietic Stem Cell Differentiation Reveals Strong
690 Erythroid Potential of Multipotent Cells. *Stem Cell Reports*. 2019;12(4):801–
691 815.
692 46. Perié L, Duffy KR, Kok L, de Boer RJ, Schumacher TN. The Branching Point in
693 Erythro-Myeloid Differentiation. *Cell*. 2015;163(7):1655–62.

694 47. Tak T, Prevedello G, Simon G, et al. Simultaneous tracking of division and
695 differentiation from individual hematopoietic stem and progenitor cells reveals
696 within-family homogeneity despite population heterogeneity. *bioRxiv*.
697 2019;586354.
698 48. Rodriguez-Fraticelli AE, Wolock SL, Weinreb CS, et al. Clonal analysis of
699 lineage fate in native haematopoiesis. *Nat. Publ. Gr.* 2018;553:.
700 49. Theurl I, Hilgendorf I, Nairz M, et al. On-demand erythrocyte disposal and iron
701 recycling requires transient macrophages in the liver. *Nat. Med.*
702 2016;22(8):945–51.
703 50. Wang J, Hayashi Y, Yokota A, et al. Expansion of EPOR-negative
704 macrophages besides erythroblasts by elevated EPOR signaling in
705 erythrocytosis mouse models. *Haematologica*. 2018;103(1):40–50.
706 51. Gilboa D, Haim-Ohana Y, Deshet-Unger N, et al. Erythropoietin enhances
707 Kupffer cell number and activity in the challenged liver. *Sci. Rep.*
708 2017;7(1):10379.
709 52. Kuzmac S, Grcevic D, Sucur A, Ivcevic S, Katavic V. Acute hematopoietic
710 stress in mice is followed by enhanced osteoclast maturation in the bone
711 marrow microenvironment. *Exp. Hematol.* 2014;42(11):966–975.
712 53. Ulyanova T, Phelps SR, Papayannopoulou T. The macrophage contribution to
713 stress erythropoiesis: when less is enough. *Blood*. 2016;128(13):1756–65.
714 54. Mausberg AK, Meyer Zu Hörste G, Dehmel T, et al. Erythropoietin ameliorates
715 rat experimental autoimmune neuritis by inducing transforming growth factor-β
716 in macrophages. *PLoS One*. 2011;6(10):e26280.
717 55. Liao C, Prabhu KS, Paulson RF. Monocyte derived macrophages expand the
718 murine stress erythropoietic niche during the recovery from anemia. *Blood*.
719 2018;blood-2018-06-856831.
720 56. Bretz CA, Divoky V, Prchal J, et al. Erythropoietin Signaling Increases
721 Choroidal Macrophages and Cytokine Expression, and Exacerbates Choroidal
722 Neovascularization. *Sci. Rep.* 2018;8(1):2161.
723 57. Kim S, Kim N, Presson AP, et al. Dynamics of HSPC repopulation in
724 nonhuman primates revealed by a decade-long clonal-tracking study. *Cell*
725 *Stem Cell*. 2014;
726 58. Aiuti A, Biasco L, Scaramuzza S, et al. Lentiviral hematopoietic stem cell gene
727 therapy in patients with wiskott-aldrich syndrome. *Science (80-.).*
728 2013;341(6148):.
729 59. Starnes LM, Sorrentino A, Pelosi E, et al. NFI-A directs the fate of
730 hematopoietic progenitors to the erythroid or granulocytic lineage and controls
731 β-globin and G-CSF receptor expression. *Blood*. 2009;114(9):1753–1763.
732 60. Meenhuis A, Van Veelen PA, De Looper H, et al. MiR-17/20/93/106 promote
733 hematopoietic cell expansion by targeting sequestosome 1-regulated pathways
734 in mice. *Blood*. 2011;118(4):916–925.
735 61. Blank U, Karlsson G, Moody JL, et al. Smad7 promotes self-renewal of
736 hematopoietic stem cells. *Blood*. 2006;
737 62. Steffen B, Knop M, Bergholz U, et al. AML1/ETO induces self-renewal in
738 hematopoietic progenitor cells via the Groucho-related amino-terminal AES
739 protein. *Blood*. 2011;117(16):4328–4337.
740 63. Wu C, Espinoza DA, Koelle SJ, et al. Geographic clonal tracking in macaques
741 provides insights into HSPC migration and differentiation. *J. Exp. Med.*
742 2018;215(1):217–232.
743 64. Sun J, Ramos A, Chapman B, et al. Clonal dynamics of native haematopoiesis.

Nature. 2014;514(7522):.
65. Busch K, Klapproth K, Barile M, et al. Fundamental properties of unperturbed haematopoiesis from stem cells in vivo. *Nature*. 2015;518(7540):542–546.
66. Schoedel KB, Morcos MNF, Zerjatke T, et al. The bulk of the hematopoietic stem cell population is dispensable for murine steady-state and stress hematopoiesis. *Blood*. 2016;128(19):2285–2296.
67. Rainville N, Jachimowicz E, Wojchowski DM. Targeting EPO and EPO receptor pathways in anemia and dysregulated erythropoiesis. *Expert Opin. Ther. Targets*. 2016;20(3):287–301.
68. Halawi R, Cappellini MD, Taher A. A higher prevalence of hematologic malignancies in patients with thalassemia: Background and culprits. *Am. J. Hematol.* 2017;92(5):414–416.

759 **Tables**

760 **Table 1: Permutation testing of changes in clonality after transplantation of EPO-**
761 **exposed HSPCs.** Same data as in Figure 1, 2, 3, 4 and Figure 7. HSPCs or MPP2
762 were cultured with different concentrations of EPO (160 ng/ml or 1,000 ng/ml) for 16h,
763 and when indicated a soluble dose of EPO (133 ug/kg) was injected together with
764 barcoded HSPCs at the moment of transplantation. Barcodes in the erythroid (E),
765 myeloid (M), B-lymphoid (B) lineage, dendritic cell (DC) and HSPCs, were analyzed
766 four weeks after transplantation and categorized by bias using a 10% threshold. For
767 the data of Figure 1, 2 and 7, the output of MB and ME classified barcodes to the B,
768 M, and E lineages was analyzed using a permutation test. For the data of Figure 3, the
769 output of MBE and MB classified barcodes to the DC lineage was analyzed. For the
770 data of Figure 4, the output of barcodes present in HSPCs to the B, M, and E lineages
771 was analyzed using a permutation test. By permutating the mice of control and EPO
772 groups, the random distribution of this output was generated and compared to the real
773 output difference between control and EPO group. A p-value was generated as in[47]

Figure	**Condition**	**p-value**			
		MB in B	**MB in M**	**ME in E**	**ME in M**
1	**HSPCs 160 ng/ml**	0.02	0.04	0.02	0.04
1, 2	**HSPCs 1000 ng/ml**	0.0075	0.0071	0.0071	0.012
2	**HSPCs 160 ng/ml + inj.**	0.01	0.016	0.012	0.011
2	**HSPCs 1000 ng/ml + inj.**	0.0018	0.0018	0.002	0.0025
7	**MPP2 1000 ng/ml**	0.006	0.008	0.004	0.004
		MBE in DC	**MB in DC**		
3	**HSPCs 1000 ng/ml**	0.07	0.0075		
		HSPC in B	**HSPC in M**	**HSPC in E**	
4	**HSPCs 160 ng/ml**	0.035	0.029	0.029	
	HSPCs 1000 ng/ml	0.008	0.06	0.01	

774

775 **Figure Legends**

776

777 **Figure 1: High output ME- and MB-biased clones occur after EPO-exposure and**
778 **transplantation of HSPCs**. **a**, HSPCs were sorted from the bone marrow of donor
779 mice, lentivirally barcoded, cultured *ex vivo* with or without 1,000 ng/ml EPO for 16 h
780 and transplanted into sublethally irradiated mice. At week 4 post-transplantation, the
781 erythroid (E), myeloid (M), and B-cells (B) lineages were sorted from the spleen and
782 processed for barcode analysis. **b**, The percentage of donor derived cells (CD45.1$^+$)
783 among the total spleen, myeloid cells (CD11b$^+$) or B-cells (CD19$^+$) in the spleen of
784 control and EPO group. **c**, To better assess chimerism in erythroid cells
785 mTdTomato/mGFP donor mice were used. The fraction of Tom$^+$ cells among erythroid
786 cells (Ter119$^+$) in the spleen and blood in control and EPO group. **d**, Number of
787 barcodes retrieved in the indicated lineages at week 4 after transplantation in control
788 and EPO group. **e**, Triangle plots showing the relative abundance of barcodes (circles)
789 in the E, M, and B lineage with respect to the summed output over the three lineages
790 (size of the circles) for control and EPO group. **f**, Percentage of HSPCs classified by
791 the indicated lineage bias, using a 10% threshold for categorization. **g**, Quantitative
792 contribution of the classes as in f to each lineage. Shown are values from several
793 animals (n= 8 EPO, n= 10 control in b, n= 3 EPO, n=4 control in c spleen, n= 4 EPO,
794 n=8 control in c blood collected over 5 different experiments (d-g) n=5 for control and
795 n=2 for EPO group collected over one experiment). For all bar graphs mean and S.D.
796 between mice are depicted. Statistical significance tested using Mann-Withney U test
797 p=0,05 for (b-c). Statistical significance tested by permutation test for different subsets
798 in g (see Table 1). This Figure has four supplements.

799

800 **Figure 2: Effect of different EPO concentrations on HSPC clonality after**
801 **transplantation.** Same protocol as in Figure 1 but HSPCs were cultured with different
802 concentrations of EPO (160 ng/ml or 1,000 ng/ml) for 16 h, and when indicated a single
803 dose of EPO (133 ug/kg) was injected together with barcoded cells at the moment of
804 transplantation. **a**, Triangle plots showing the relative abundance of barcodes (circles)
805 in the erythroid (E), myeloid (M), and B-lymphoid (B) lineage with respect to the
806 summed output over the three lineages (size of the circles) for the different
807 experimental groups as indicated. **b**, The percentage of each lineage produced by the
808 barcodes categorized by bias using a 10% threshold. Shown are values from several
809 animals (n=2 for 160 ng/ml, 1,000 ng/ml, and 160 ng/ml + EPO injection, n=4 for 1,000
810 ng/ml + EPO injection (collected over 4 different experiments)). For all bar graphs
811 mean and S.D. between mice are depicted. Statistical significance tested by
812 permutation test for different subsets in b (see Table 1). This figure has one
813 supplement.
814
815 **Figure 3: Production of Dendritic Cells (DC) and Megakaryocyte Progenitors**
816 **(MkP) by HSPCs after EPO-exposure and transplantation.** In addition to the
817 analysis of barcodes in the erythroid (E), the myeloid (M), and the B-cell (B) lineage,
818 the DC lineage in spleen and MkP in bone marrow were added. **a**, Percentage of
819 barcoded HSPCs producing DC in the different HSPC categories (classification as in
820 Figure 2 based on the M, E, and B lineage only using a 10% threshold. The DC only
821 category was added). **b**, The percentage of the DC lineage produced by the barcodes
822 categorized by bias as in a. **c-d**, Representations as in a-b for barcode detection in
823 MkP. Data is derived from a cohort with detailed myeloid sorting. The myeloid lineage
824 was merged according to the percentage of total donor myeloid each subset

825 contributed as in Figure 2 – supplement 1a to allow classification as in a-b based on
826 the M, E, and B lineage only using a 10% threshold. The MkP only category was added.
827 Shown are values from several animals (a-b, n=5 for control and n=2 for EPO group,
828 c-d, n=3 for control and n=1 for EPO group (collected over two experiments)). For all
829 bar graphs mean and S.D. between mice are depicted. Statistical significance tested
830 using Mann-Withney U test p=0,05 for (a,c). Statistical significance tested by
831 permutation test for different subsets in b (see Table 1). This figure has one
832 supplement.
833
834 **Figure 4: Overlap of barcodes in HSPCs and mature cells after transplantation**
835 **of EPO-exposed HSPCs.** Same protocol as in Figure 1 but HSPCs were cultured with
836 two different concentrations of EPO (160 ng/ml or 1000 ng/ml) for 16 h. In addition,
837 HSPCs were sorted and subjected to barcode analysis. **a**, The total number of
838 barcodes found back in HSPCs. **b**, The percentage of barcodes in the mature cell
839 subsets also detected in HSPCs and the percentage of barcodes in HSPCs also
840 detected in mature cells. **c**, The percentage of the HSPC lineage contributed by
841 barcodes categorized by bias as in Figure 2 based on the M, E, and B lineage using a
842 10% threshold. **d**, The percentage of each lineage produced by the barcodes color
843 coded for presence (blue) and absence (grey) in HSPCs. Shown are values from
844 several animals (n=5 for control, n=2 for EPO 160 ng/ml group and n=3 for EPO 1,000
845 ng/ml group). For all bar graphs mean and S.D. between mice are depicted. Statistical
846 significance tested using Mann-Withney U test p=0,05 for (a-b). Statistical significance
847 tested by permutation test for different subsets in d (see Table 1).
848

849 **Figure 5: Characterization of EPO-exposed HSPCs by scRNAseq.** HSPCs were
850 sorted, barcoded and cultured *ex vivo* with or without 1,000 ng/ml EPO for 16 h, and
851 analysed by scRNAseq using the 10X Genomics platform. 1,706 cells from control and
852 1,595 cells from EPO group passed quality control **a**, Volcano plot of log2 fold change
853 of the differentially expressed genes between control and EPO-exposed cells versus
854 the adjusted p-value. Genes of interest are annotated. Differentially expressed genes
855 were used to defined an EPO response signature. **b**, UMAP visualization of the EPO-
856 exposed and control HSPCs. **c**, The level of expression in the EPO-exposed HSPCs
857 of the genes in the EPO response signature (top), and definition of the EPO-responder
858 and non-responder subgroups using the 90th percentile expression of the EPO
859 response signature from c (bottom). **d**, The expression of the indicated genes in the
860 control, EPO-responder and non-responder subgroups as defined in c. Genes that are
861 significantly upregulated in the EPO-responder group, when compared to control and
862 non-responder groups. Differential expression was assessed using a logistic
863 regression testing approach, as implemented in Seurat. This figure has two
864 supplements and correspond to one 10X experiment of a pool of 8 mice.
865
866 **Figure 6: EPO-responders are multipotent progenitors, not HSCs.** Same protocol
867 as in Figure 5**. a,** Expression of published gene-signatures of HSCs (dormant HSC[40],
868 molecular overlap (molO) HSC signature[41]) and MPPs (MPP1[40]-2[31]) across the entire
869 dataset (see Methods) **b**, Expression of the signatures from 6a, across control, non-
870 responder, and EPO-responder groups as defined in Figure 5c. Statistical comparisons
871 made using a Kruskal Wallis Test with a Dunns multiple comparisons post-hoc test **c**,
872 Expression of the molO HSC signature on the published reference map[42]. **d**, Nearest-

873 neighbor mapping of control, EPO-responder and non-responder cells onto the
874 published reference map[42].
875
876 **Figure 7: MPP2 are enriched for ME-biased clones after EPO-exposure and**
877 **transplantation.** MPP2 and CD48$^-$ HSPCs were sorted from the bone marrow of donor
878 mice, MPP2 were lentivirally barcoded, and both populations cultured *ex vivo* with or
879 without 1,000 ng/ml EPO for 16 h. After the culture, barcoded MPP2 and un-barcoded
880 CD48$^-$ HSPCs were mixed and transplanted into sublethally irradiated mice. At week
881 4 post-transplantation, the erythroid (E), myeloid (M), and B-cells (B) lineages were
882 sorted from the spleen and processed for barcode analysis. **a**, The fraction of donor
883 cells among the indicated cell types in spleen. **b**, Barcode number retrieved in the
884 indicated lineage at 4 weeks after transplantation in control and EPO 1,000 ng/ml
885 group. **c**, Percentage of MPP2s classified using a threshold of 10% in experimental
886 groups as indicated. **d**, The percentage of each lineage produced by the MPP2
887 barcodes categorized by bias using a 10% threshold. **e**, Triangle plots showing the
888 relative abundance of barcodes (circles) in the erythroid (E), myeloid (M), and B-
889 lymphoid (B) lineage with respect to the summed output over the three lineages (size
890 of the circles). Shown are data from several mice (n=3 for control and n=4 for EPO
891 group). For all bar graphs mean and S.D. between mice are depicted. Statistical
892 significance tested using Mann-Withney U test p=0,05 for (c-e). Statistical significance
893 tested by permutation test for different subsets in a (see Table 1). This figure has one
894 supplement.
895
896 **Figure 8: The effect of EPO on HSPC clonality after transplantation is transient.**
897 Same protocol as in Figure 1, but barcodes in the E, M, and B lineage in spleen of

898 individual mice sacrificed at month 4 post-transplantation were analyzed. **a**, Triangle
899 plots showing the relative abundance of barcodes (circles) in the erythroid (E), myeloid
900 (M), and B-cell (B) lineage with respect to the summed output over the three lineages
901 (size of the circles) for the different experimental groups as indicated. **b**, The
902 percentage of each lineage produced by the barcodes categorized by bias using a
903 10% threshold. **c**, The fraction of donor cells among the indicated cell types in spleen.
904 **d**, Barcode number retrieved in the indicated lineage at month 4 after transplantation
905 in control, EPO 160 ng/ml, and EPO 1,000 ng/ml group. **e**, Percentage of HSPCs
906 classified using a threshold of 10% in experimental groups as indicated. Shown are
907 data from several mice. (c, n=5 for control and n=4 for each EPO group, (a-b, d-e) n=6
908 for control and n=4 for each EPO group (collected over two experiments)). For all bar
909 graphs mean and S.D. between mice are depicted. Statistical significance tested using
910 Mann-Withney U test p=0,05 for (c-e).
911
912 **Figure supplements legends**
913
914 **Figure 1 – figure supplement 1: Gating strategies and HSPC marker expression**
915 **after lentiviral transduction and *ex vivo* culture with or without EPO. a**, HSPCs
916 were gated as propidium iodide negative single C-Kit$^+$ Sca-1$^+$ Flt3$^-$ CD150$^+$ cells of C-
917 Kit$^+$ enriched bone marrow cells. **b**, Erythroblast cells were gated as Ter119$^+$ CD44$^+$
918 FSC^{hi} cells on Ter$^+$ enriched cells. **c**, Gating strategy for B-cells (CD19$^+$ CD11b$^-$),
919 dendritic cells (CD19$^-$ CD11b$^-$ CD11c$^+$), and myeloid cells (CD119$^-$ CD11c$^-$ CD11b$^+$) on
920 Ter119$^-$ live single donor cells. **d**, Gating for MkP (C-Kit$^+$ Sca-1$^-$ CD150$^+$ CD41$^+$) from
921 C-Kit$^+$ enriched bone marrow cells. **e**, Sort gating for GFP$^+$ erythroid, myeloid, B-, and
922 dendritic cells respectively used for barcoding analysis. **f**, Representative flow

923 cytometry plots of sorted HSPC pool after 6 h lentiviral transduction and 16 h *ex vivo*
924 incubation with or without EPO.

925 **Figure 1 – figure supplement 2: Correlations in barcoding profiles of spleen and**
926 **bone.** HSPCs were sorted from the bone marrow of donor mice, lentivirally barcoded,
927 cultured *ex vivo* for 16 h and transplanted into sublethally irradiated mice. At week 4
928 post-transplantation, erythroid (E), B-cells (B), and the myeloid lineage (M) cells
929 monocytes, eosinophils, neutrophils, and macrophages were sorted from the spleen
930 and from bone and processed for barcode analysis. The myeloid lineage was merged
931 according to the percentage of total donor myeloid each subset contributed as in
932 Supplementary Figure 4a. **a**, Heatmaps showing the output of individual barcodes
933 (rows) in different samples (columns) as indicated. Data is normalized by cell subset,
934 log transformed, and clustered by complete linkage using Euclidean distance. No
935 output is represented in black. **b**, The percentage of barcodes in spleen and bone
936 detected in the respective other organ. The spearman rank correlation of barcodes in
937 bone and spleen was for the B-, M- and E-lineage 0.81, 0,69 and 0,7 respectively.
938 Shown are values from several animals (n= 3). For all bar graphs mean and S.D.
939 between mice are depicted. Statistical significance tested using Mann-Withney U test
940 p=0,05 for (b).

941

942 **Figure 1 – figure supplement 3: Characterization of lineage biases after**
943 **transplantation of EPO-exposed HSPCs**. **a**, Triangle plots from Figure 1e color
944 coded by mice. **b**, Quantitative contribution of the classes to each lineage as in Figure
945 1 using different thresholds of 0%, 5%, 10%, 15% and 20%. **c-f**, Data for an additional
946 experiment as in Figure 1. **c**, Number of barcodes retrieved in the indicated lineages

947 at week 4 after transplantation in control and EPO group. **d**, Triangle plots showing the
948 relative abundance of barcodes (circles) in the erythroid (E), myeloid (M), and B-cell
949 (B) lineage with respect to the summed output over the three lineages (size of the
950 circles) for control and EPO group. **e**, Proportion of HSPCs classified in the indicated
951 lineage bias category, using a 10% classification threshold. **f**, Quantitative contribution
952 of the classes as in f to each lineage. Shown are values from several animals (a-c, n=5
953 for control group and n=2 for EPO group (collected over one experiment), d-f, n= 2 for
954 control, n= 3 for EPO group (collected over one experiment)). For all bar graphs mean
955 and S.D. between mice are depicted. Statistical significance tested using Mann-
956 Withney U test p=0,05 for (c, e).

957 **Figure 1 – figure supplement 4: High output ME- and MB-biased HSPCs occur**
958 **six weeks after transplantation of EPO-exposed HSPCs.** HSPCs were sorted from
959 the bone marrow of donor mice, lentivirally barcoded, cultured *ex vivo* with or without
960 1,000 ng/ml EPO for 16 h and transplanted into sublethally irradiated mice. At week 6
961 post-transplantation, the erythroid (E), myeloid (M), and B-cells (B) lineages were
962 sorted from the spleen and processed for barcode analysis. Quantitative contribution
963 of HSPCs classified by the indicated lineage bias, using a 10% threshold for
964 categorization, to each lineage. Shown are values from several animals (n= 2 EPO, n=
965 4 control). Mean and S.D. between mice are depicted.

966 **Figure 2 – figure supplement 1: Variability in the effect of different EPO**
967 **concentrations on clonality after HSPC transplantation at different timepoints. a**,
968 Triangle plots showing the relative abundance of barcodes (circles) in the erythroid (E),
969 myeloid (M), and B-cell (B) lineage with respect to the summed output over the three

970 lineages (size of circles) for control and EPO groups of Figure 2, color coded by mice.
971 **b**, Same representation as in a for data of Figure 8.

972 **Figure 3 – figure supplement 1: Production of macrophages, monocytes,**
973 **neutrophils, eosinophils, and Megakaryocyte Progenitors (MkP) by HSPCs after**
974 **EPO-exposure and transplantation**. Same experimental protocol as in Figure 1 but
975 the myeloid cells were subdivided into monocytes, eosinophils, macrophages and
976 neutrophils, and MkP were sorted. **a**, Gating for detailed myeloid subsets on myeloid
977 cells. Monocytes (Mo) were sorted as $CD115^+$ cells, eosinophils (Eo) as $CD115^-$
978 $SiglecF^+$ $Ly6G^+$, macrophages (Ma) as $CD115^-$ $SiglecF^-$ $Ly6G^-$, and neutrophils (Neu)
979 as $CD115^-$ $SiglecF^-$ $Ly6G^+$ cells. **b**, The contribution of different cell types to the overall
980 donor myeloid subset in control and EPO group. **c**, Heatmaps showing the output of
981 individual barcodes (rows) in different samples (columns) as indicated. Data is
982 normalized by cell subset, log transformed, and clustered by complete linkage using
983 Euclidean distance. No output is represented in black. Shown are values from several
984 animals (b, n=5 for control and n= 3 for EPO group c, n=3 for control and n=2 for EPO
985 group (collected over two experiments)). For all bar graphs mean and S.D. between
986 mice are depicted. Statistical significance tested using Mann-Withney U test p=0,05
987 for (b).

988

989 **Figure 5 – figure supplement 1: ScRNAseq analysis of control and EPO-exposed**
990 **HSPCs a,** UMAP projection of the scRNAseq dataset from[42] annotated with *flt3*,
991 *CD150*, and *gata1* gene expression. **b**, Projecting of erythroid-biased progenitors
992 from[10] on UMAP projection of a. **c**, Robustness of the UMAP visualization and
993 unsupervised clustering of the data in Figure 4c .The amount of variance explained by

994 each principle component (left) and UMAP-based visualization using 10 PCA (right)
995 for different number of genes. **d**, The expression of genes encoding known EPO
996 receptors in each subgroup. **e,** Overview of the reference map using supervised cell
997 type annotation of the dataset from[42]. On the right hand side we overlay the MPP4
998 signature defined by[31] onto our reference map to facilitate celltype annotation **f**, HSPCs
999 were sorted, barcoded and cultured *ex vivo* with or without 1,000 ng/ml EPO for 16 h,
1000 and analysed by scRNAseq using the 10X Genomics platform. Mapping of the
1001 transcriptomes of the 1,706 cells from control and 1,595 cells from EPO group obtained
1002 after quality control onto the reference map using a k-nearest neighbors mapping
1003 approach.
1004
1005 **Figure 5 – figure supplement 2: Unsupervised clustering of control and EPO-**
1006 **exposed HSPCs a,** Cluster stability analysis varying the resolution parameter of the
1007 Seurat clustering method. The significant variable genes using 10 PCA were used as
1008 input. **b**, UMAP visualization of the data in a using a clustering resolution of 0.1. with
1009 the proportion of each cluster as in the control, EPO-responder and non-responder
1010 subgroups. **c**, expression of published signatures of established celltypes used to
1011 annotate our clusters. All comparisons in signature expression between clusters were
1012 statistically significant (adjusted p-value < 0.05) as determined by a Kruskal-Wallis
1013 Test and Dunns Post-Hoc analysis. **d**, Nearest neighbor mapping of unsupervised
1014 clusters from b onto the reference map.
1015
1016 **Figure 7 – figure supplement 1: Characterization of lineage biases after**
1017 **transplantation of EPO-exposed MPP2**. **a**, MPP2s and $CD48^-$ HSPCs were gated as
1018 propidium iodide negative single $C\text{-}Kit^+$ $Sca\text{-}1^+$ $Flt3^-$ $CD150^+$ $CD48^+$ (MPP2) and $CD48^-$

1019 (CD48$^-$ HSPCs) cells of C-Kit$^+$ enriched bone marrow cells. **b**, Triangle plots from
1020 Figure 7b color coded by mice. **c**, Quantitative contribution of the classes to each
1021 lineage as in Figure 7a using different thresholds of 0%, 5%, 10%, 15% and 20%. (a-
1022 c, n=5 for control group and n=2 for EPO group (collected over one experiment).
1023 Shown are values from several animals (n= 3 for control, n= 4 for EPO group (collected
1024 over one experiment)). For all bar graphs mean and S.D. between mice are depicted.
1025
1026 The article has one Supplementary File 1**.**
1027
1028 **Supplementary File legends:**
1029
1030 **Supplementary File 1.** Permutation testing of changes in clonality after transplantation
1031 of EPO-exposed HSPCs**.** Same data as in Figure 1 figure supplement 4 and Figure 1
1032 figure supplement 3. HSPCs were cultured with EPO (1,000 ng/ml) for 16h. Barcodes
1033 in the erythroid (E), myeloid (M), B-lymphoid (B) lineage, dendritic cell (DC) and
1034 HSPCs, were analyzed four weeks after transplantation and categorized by bias using
1035 a 10% threshold. The output of MB and ME classified barcodes to the B, M, and E
1036 lineages was analyzed using a permutation test. By permutating the mice of control
1037 and EPO groups, the random distribution of this output was generated and compared
1038 to the real output difference between control and EPO group. A p-value was generated
1039 by permutation testing.
1040

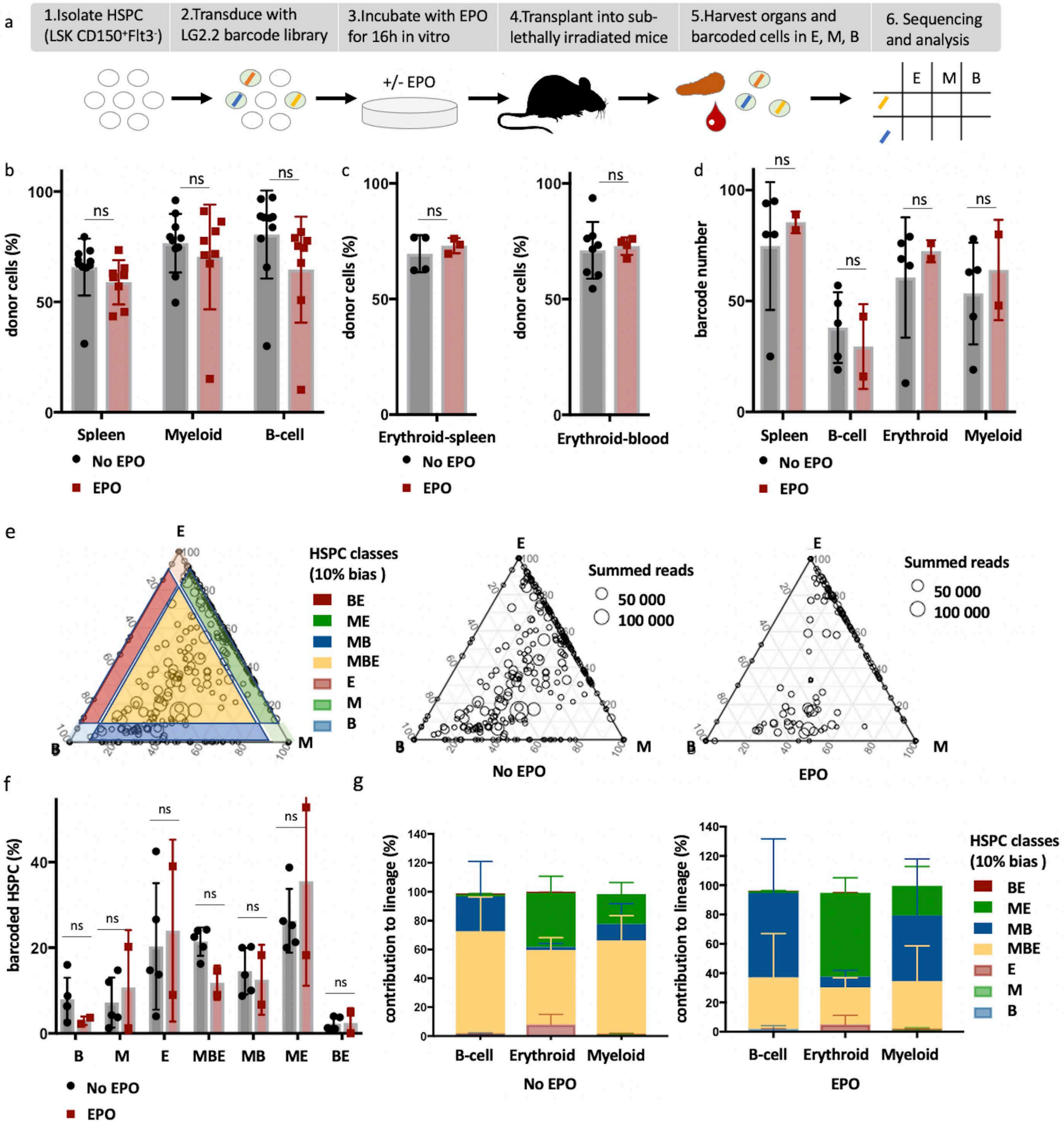
a
1.Isolate HSPC (LSK CD150+Flt3-)
2.Transduce with LG2.2 barcode library
3.Incubate with EPO for 16h in vitro
4.Transplant into sub-lethally irradiated mice
5.Harvest organs and barcoded cells in E, M, B
6. Sequencing and analysis
+/- EPO
E
M
B
b
donor cells (%)
ns
Spleen
Myeloid
B-cell
No EPO
EPO
c
donor cells (%)
Erythroid-spleen
Erythroid-blood
d
barcode number
Spleen
B-cell
Erythroid
Myeloid
e
HSPC classes (10% bias)
BE
ME
MB
MBE
E
M
B
Summed reads
50 000
100 000
No EPO
EPO
f
barcoded HSPC (%)
B
M
E
MBE
MB
ME
BE
No EPO
EPO
g
contribution to lineage (%)
B-cell
Erythroid
Myeloid
No EPO
EPO
HSPC classes (10% bias)
BE
ME
MB
MBE
E
M
B

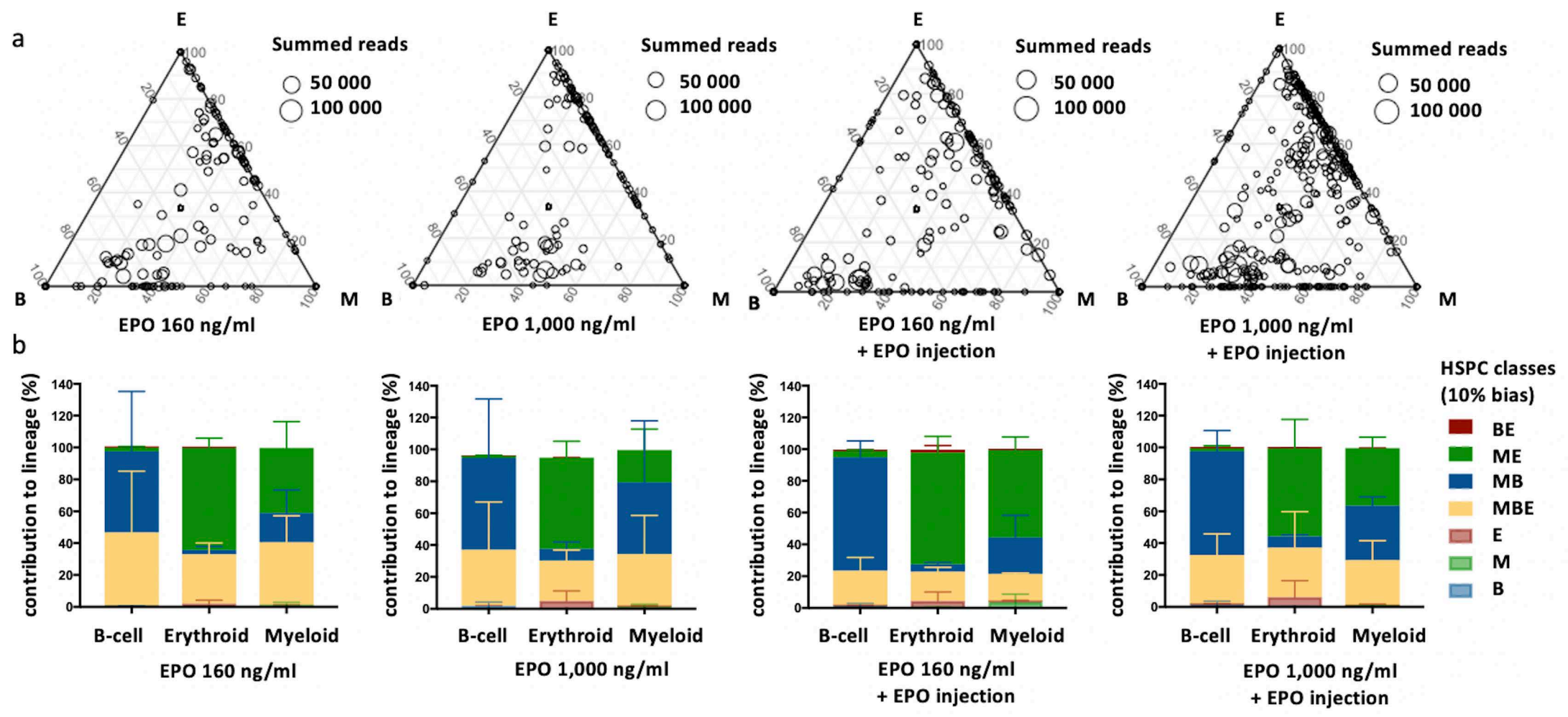
a
E
B
M
Summed reads
50 000
100 000
EPO 160 ng/ml
EPO 1,000 ng/ml
EPO 160 ng/ml
+ EPO injection
EPO 1,000 ng/ml
+ EPO injection
b
contribution to lineage (%)
B-cell
Erythroid
Myeloid
HSPC classes
(10% bias)
BE
ME
MB
MBE
E
M
B

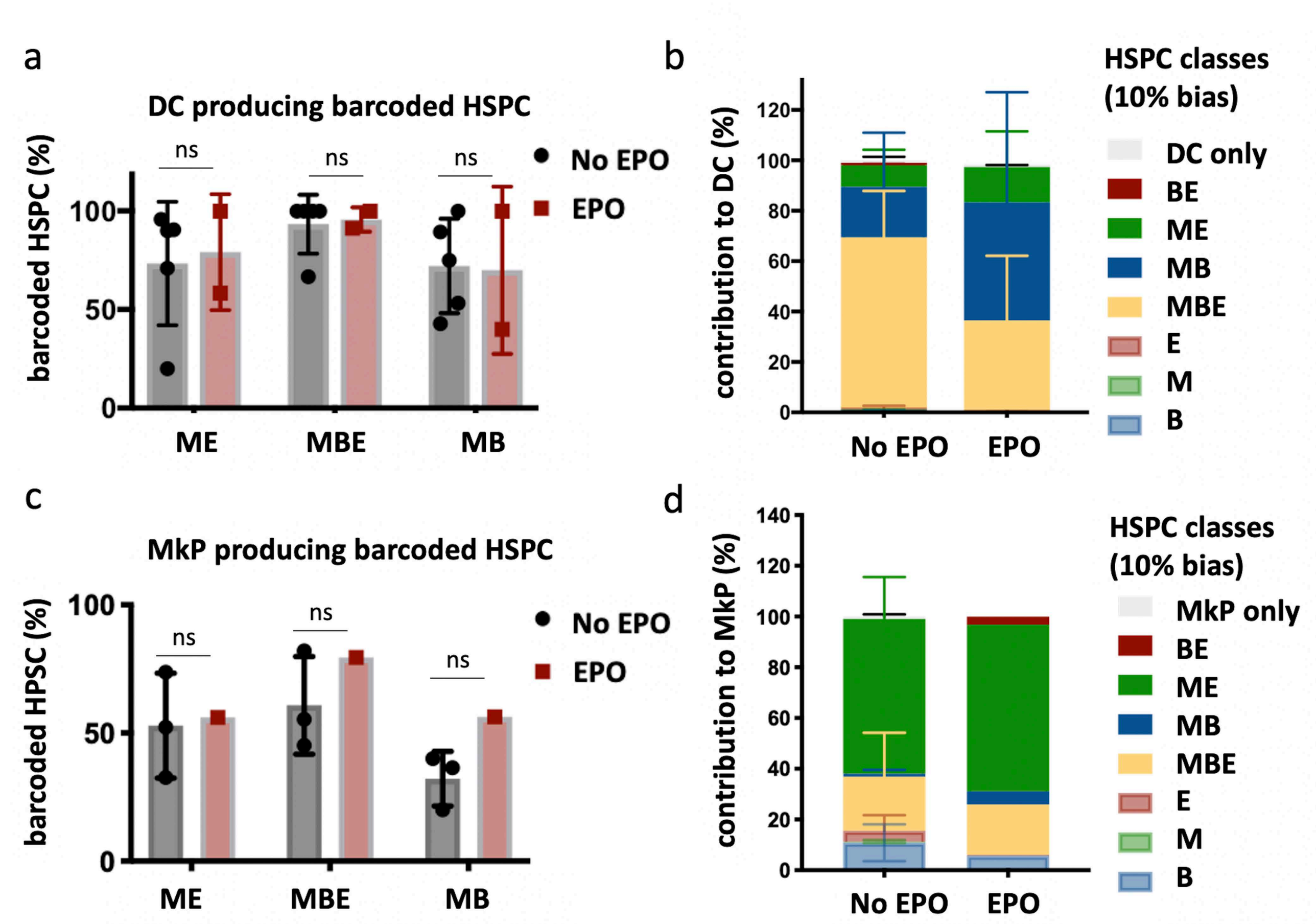
a
DC producing barcoded HSPC
barcoded HSPC (%)
100
50
0
ns
ns
ns
ME
MBE
MB
No EPO
EPO
b
contribution to DC (%)
120
100
80
60
40
20
0
No EPO
EPO
HSPC classes
(10% bias)
DC only
BE
ME
MB
MBE
E
M
B
c
MkP producing barcoded HSPC
barcoded HPSC (%)
100
50
0
ns
ns
ns
ME
MBE
MB
No EPO
EPO
d
contribution to MkP (%)
140
120
100
80
60
40
20
0
No EPO
EPO
HSPC classes
(10% bias)
MkP only
BE
ME
MB
MBE
E
M
B

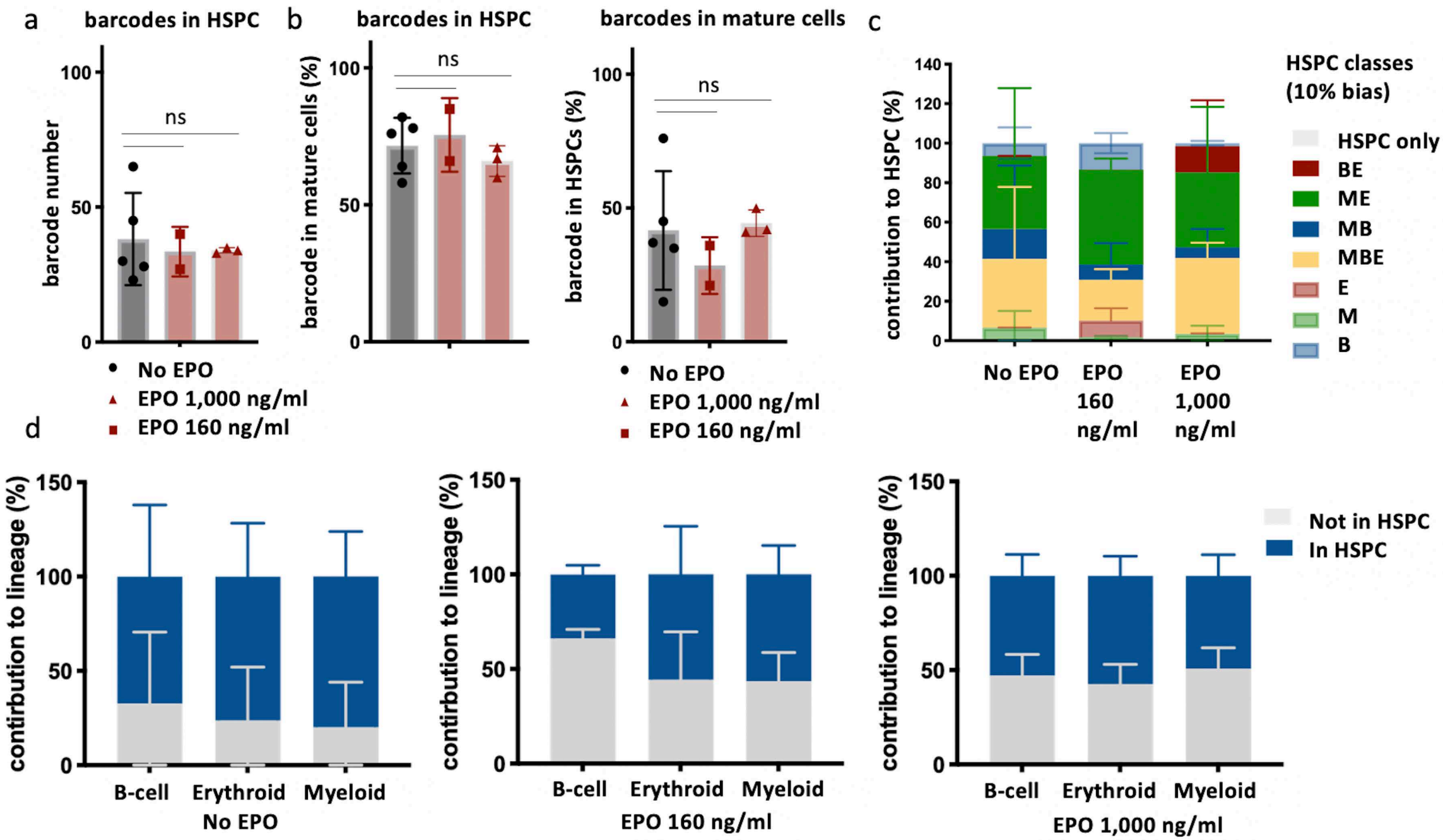
a
barcodes in HSPC
barcode number
ns
No EPO
EPO 1,000 ng/ml
EPO 160 ng/ml
b
barcodes in HSPC
barcode in mature cells (%)
ns
barcodes in mature cells
barcode in HSPCs (%)
ns
No EPO
EPO 1,000 ng/ml
EPO 160 ng/ml
c
contribution to HSPC (%)
No EPO
EPO 160 ng/ml
EPO 1,000 ng/ml
HSPC classes (10% bias)
HSPC only
BE
ME
MB
MBE
E
M
B
d
contribution to lineage (%)
B-cell
Erythroid
Myeloid
No EPO
EPO 160 ng/ml
EPO 1,000 ng/ml
Not in HSPC
In HSPC

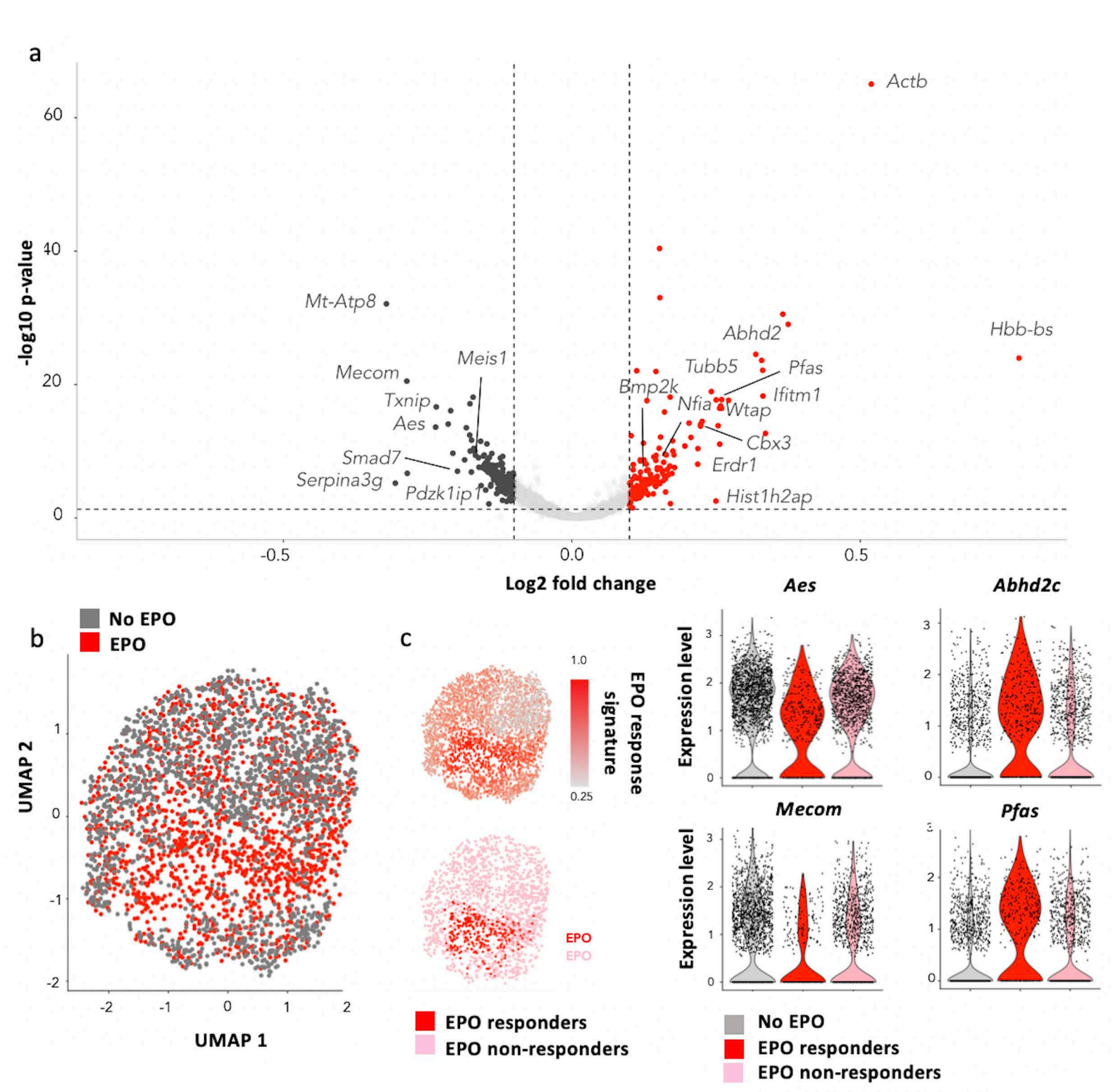
a
Actb
Mt-Atp8
Hbb-bs
Abhd2
Meis1
Tubb5
Pfas
Mecom
Bmp2k
Ifitm1
Txnip
Nfia
Wtap
Aes
Cbx3
Smad7
Erdr1
Serpina3g
Pdzk1ip1
Hist1h2ap
-log10 p-value
Log2 fold change
b
No EPO
EPO
UMAP 2
UMAP 1
c
EPO response signature
1.0
0.25
EPO
EPO
EPO responders
EPO non-responders
Aes
Abhd2c
Mecom
Pfas
Expression level
No EPO
EPO responders
EPO non-responders

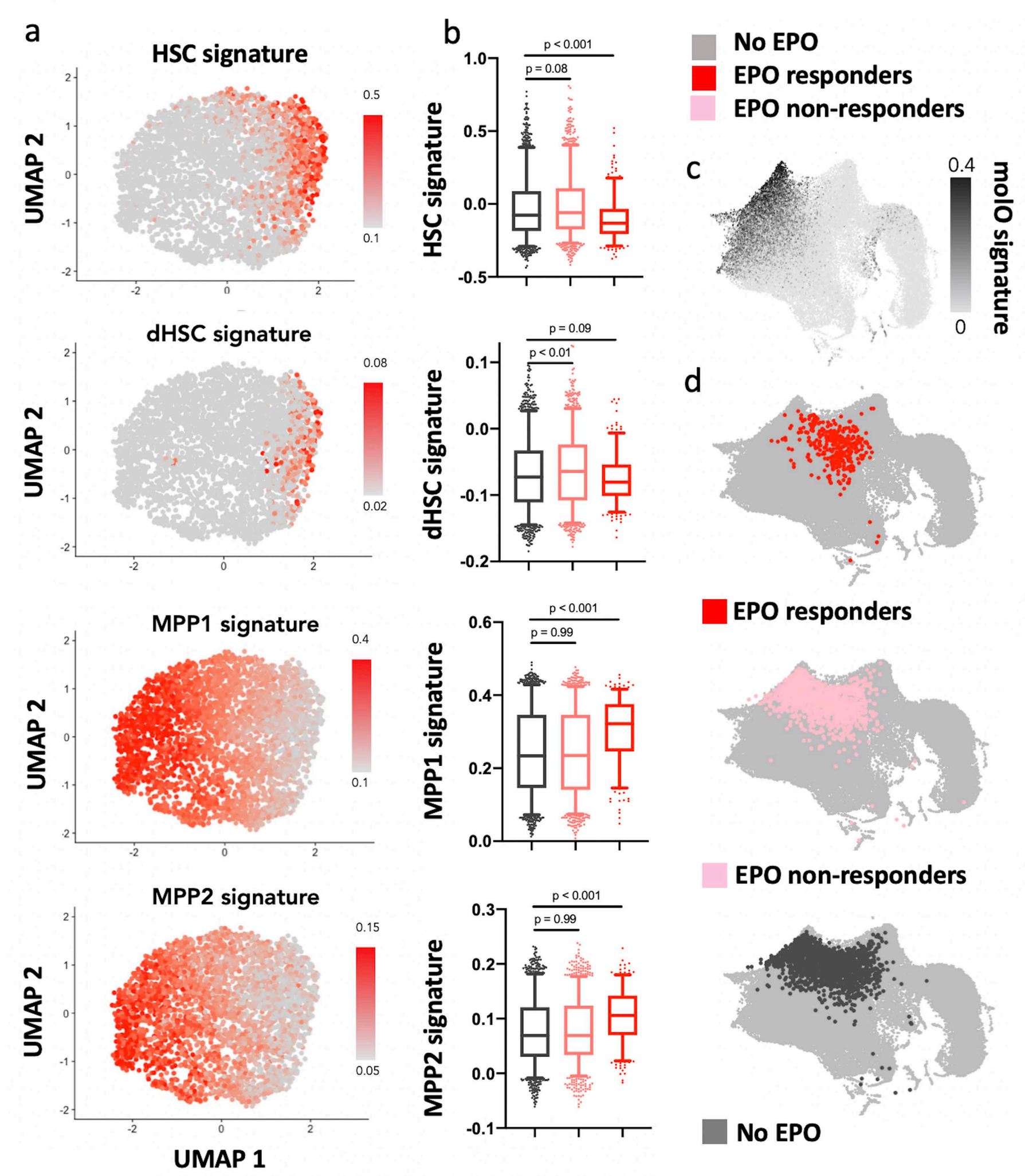
a
HSC signature
0.5
0.1
UMAP 2
dHSC signature
0.08
0.02
MPP1 signature
0.4
0.1
MPP2 signature
0.15
0.05
UMAP 1
b
p < 0.001
p = 0.08
HSC signature
p = 0.09
p < 0.01
dHSC signature
p < 0.001
p = 0.99
MPP1 signature
p < 0.001
p = 0.99
MPP2 signature
No EPO
EPO responders
EPO non-responders
c
0.4
0
molO signature
d
EPO responders
EPO non-responders
No EPO

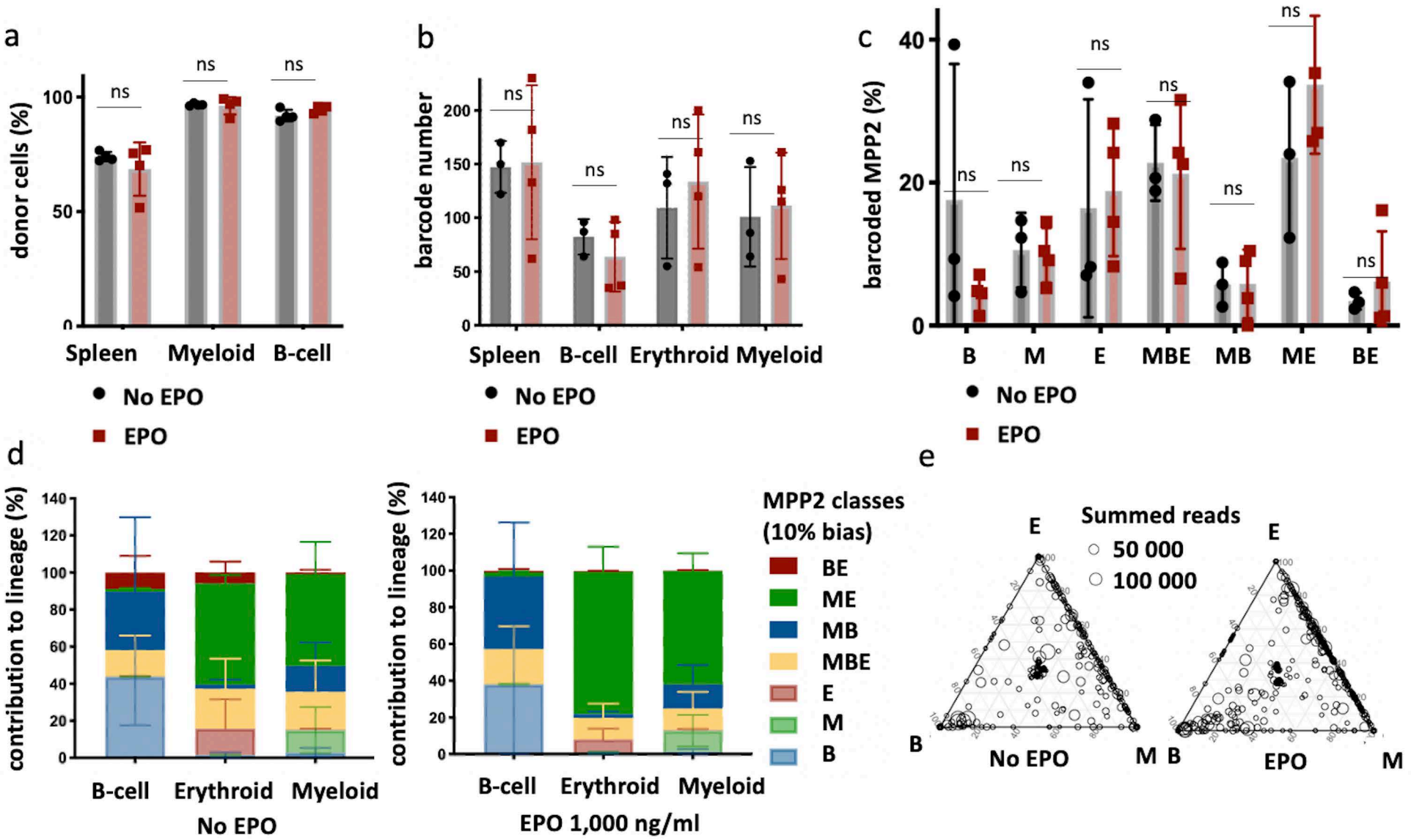
a
donor cells (%)
100
50
0
ns
ns
ns
Spleen
Myeloid
B-cell
No EPO
EPO
b
barcode number
200
150
100
50
0
ns
ns
ns
ns
Spleen
B-cell
Erythroid
Myeloid
No EPO
EPO
c
barcoded MPP2 (%)
40
20
0
ns
ns
ns
ns
ns
ns
ns
B
M
E
MBE
MB
ME
BE
No EPO
EPO
d
contribution to lineage (%)
140
120
100
80
60
40
20
0
B-cell
Erythroid
Myeloid
No EPO
EPO 1,000 ng/ml
MPP2 classes
(10% bias)
BE
ME
MB
MBE
E
M
B
e
Summed reads
50 000
100 000
E
B
M
No EPO
EPO

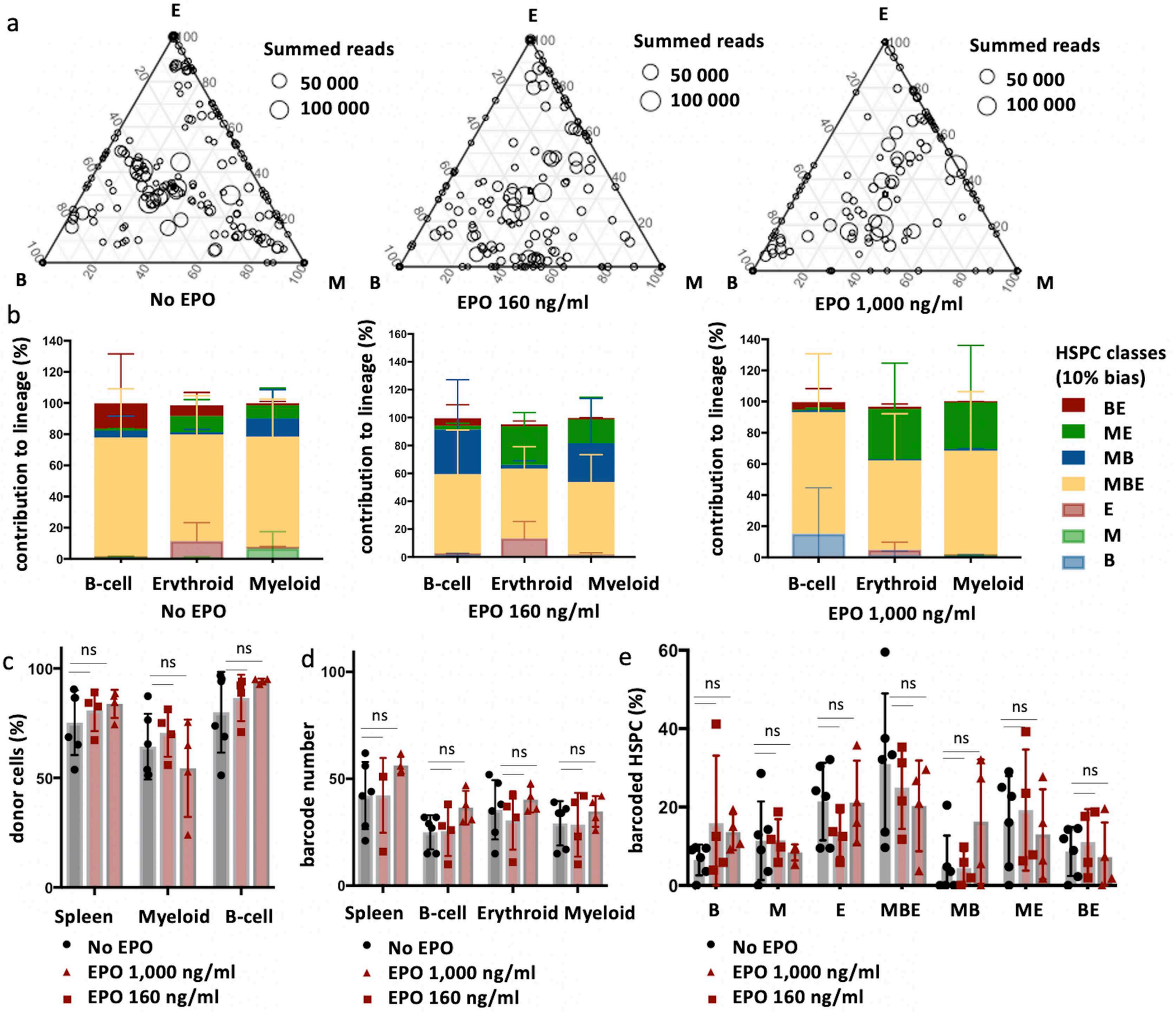
a
E
B
M
Summed reads
50 000
100 000
No EPO
EPO 160 ng/ml
EPO 1,000 ng/ml
b
contribution to lineage (%)
B-cell
Erythroid
Myeloid
HSPC classes
(10% bias)
BE
ME
MB
MBE
E
M
B
c
donor cells (%)
ns
Spleen
Myeloid
B-cell
No EPO
EPO 1,000 ng/ml
EPO 160 ng/ml
d
barcode number
Spleen
B-cell
Erythroid
Myeloid
e
barcoded HSPC (%)
B
M
E
MBE
MB
ME
BE

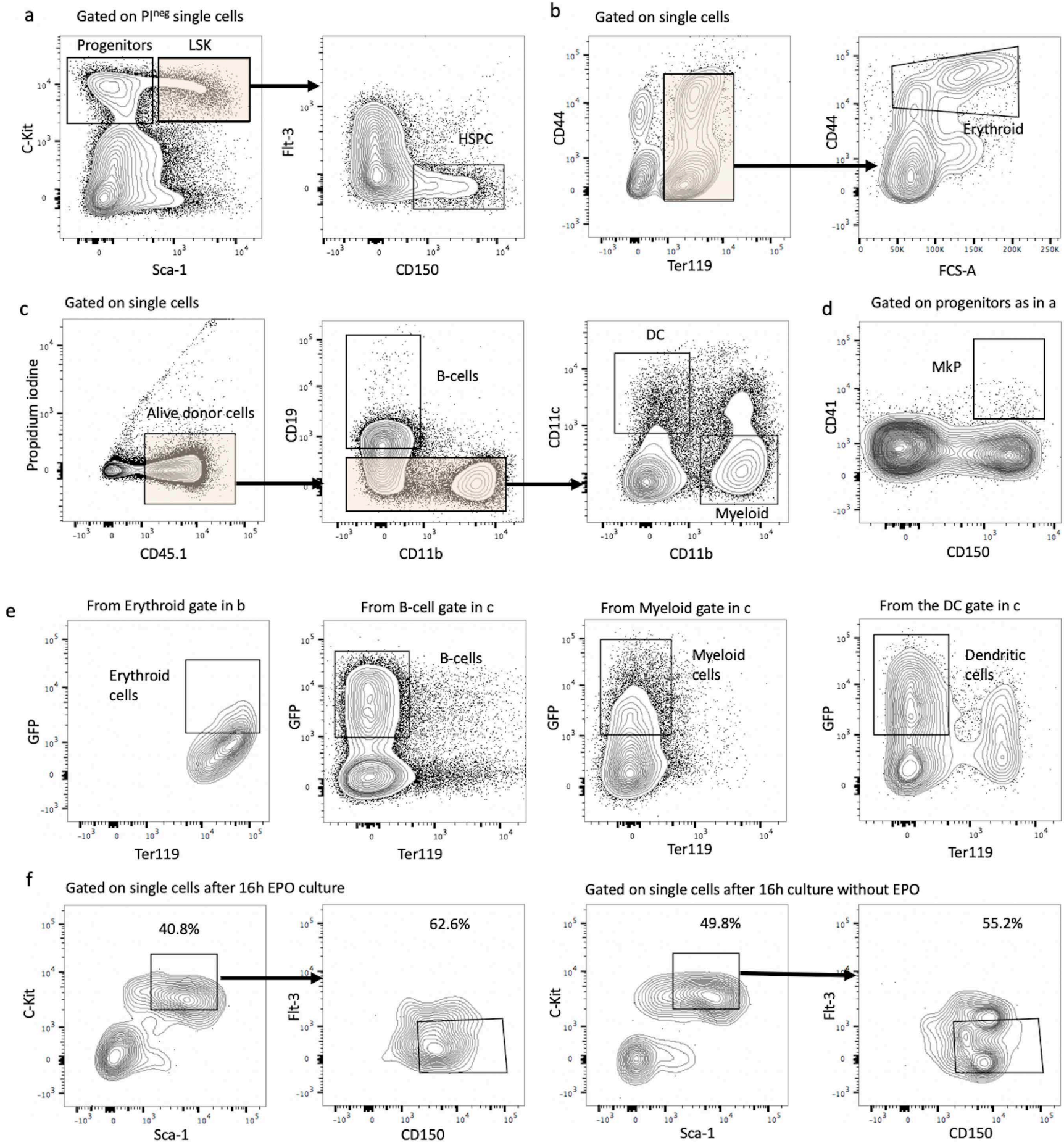
a
Gated on PI^neg single cells
Progenitors
LSK
C-Kit
Sca-1
Flt-3
CD150
HSPC
b
Gated on single cells
CD44
Ter119
Erythroid
FCS-A
c
Gated on single cells
Propidium iodine
CD45.1
Alive donor cells
CD19
CD11b
B-cells
CD11c
DC
Myeloid
d
Gated on progenitors as in a
CD41
CD150
MkP
e
From Erythroid gate in b
From B-cell gate in c
From Myeloid gate in c
From the DC gate in c
GFP
Ter119
Erythroid cells
B-cells
Myeloid cells
Dendritic cells
f
Gated on single cells after 16h EPO culture
Gated on single cells after 16h culture without EPO
40.8%
62.6%
49.8%
55.2%
C-Kit
Sca-1
Flt-3
CD150

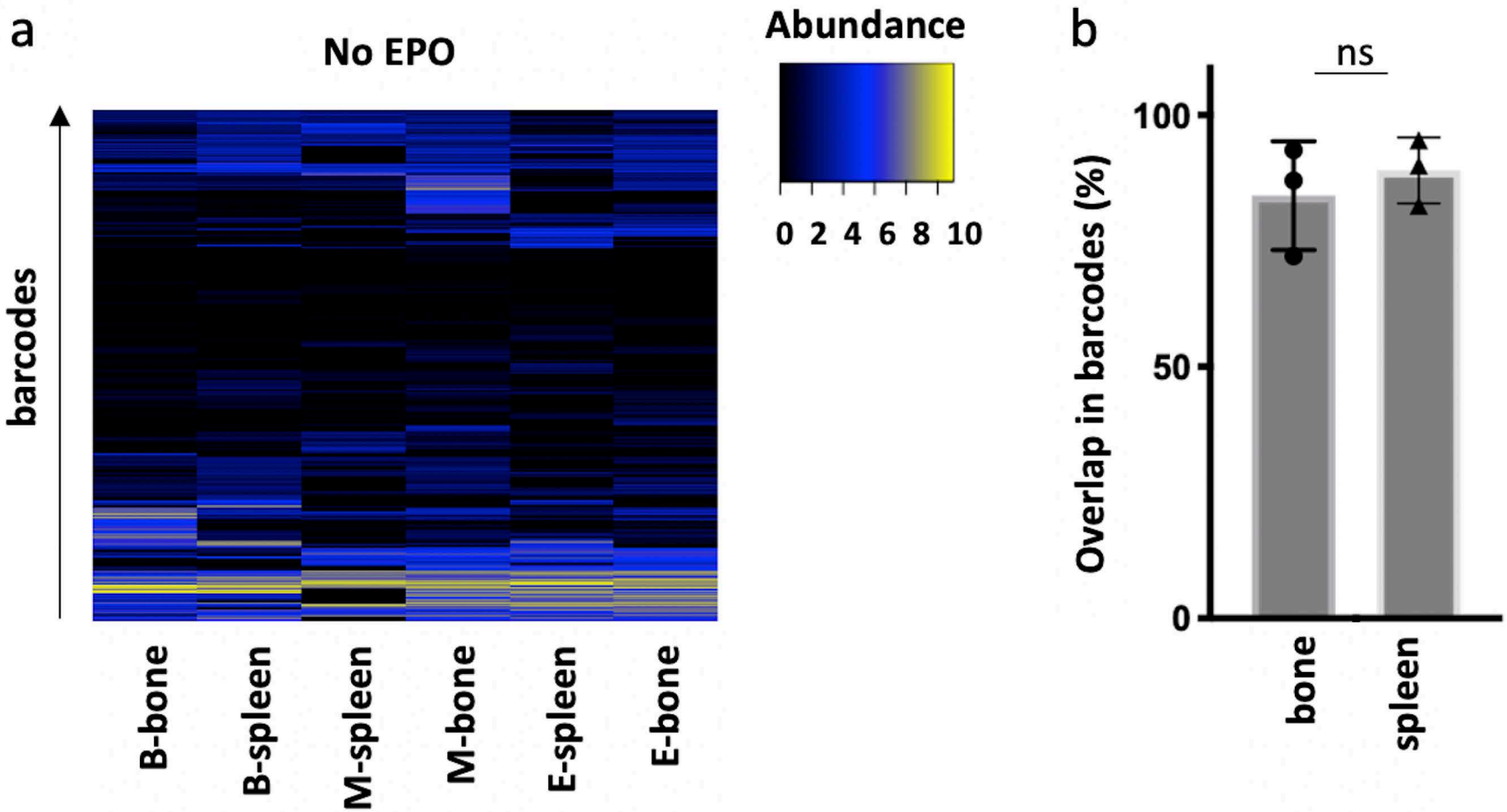
a
No EPO
Abundance
0 2 4 6 8 10
barcodes
B-bone
B-spleen
M-spleen
M-bone
E-spleen
E-bone
b
ns
Overlap in barcodes (%)
100
50
0
bone
spleen

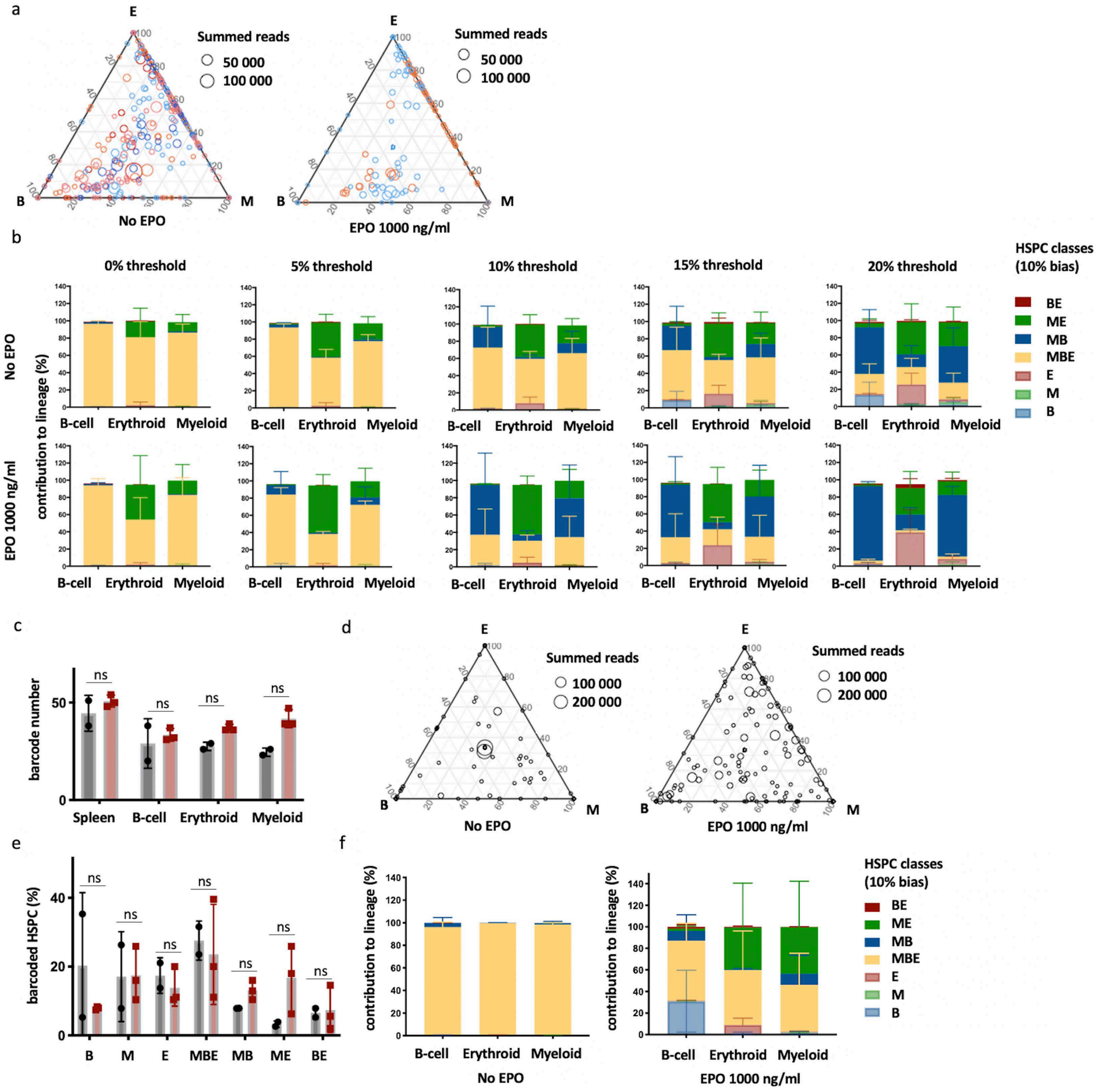
a
E
B
M
Summed reads
50 000
100 000
No EPO
EPO 1000 ng/ml
b
0% threshold
5% threshold
10% threshold
15% threshold
20% threshold
HSPC classes
(10% bias)
BE
ME
MB
MBE
E
M
B
No EPO
EPO 1000 ng/ml
contribution to lineage (%)
B-cell
Erythroid
Myeloid
c
barcode number
ns
Spleen
B-cell
Erythroid
Myeloid
d
Summed reads
100 000
200 000
No EPO
EPO 1000 ng/ml
e
barcoded HSPC (%)
B
M
E
MBE
MB
ME
BE
f
contribution to lineage (%)
B-cell
Erythroid
Myeloid
No EPO
EPO 1000 ng/ml

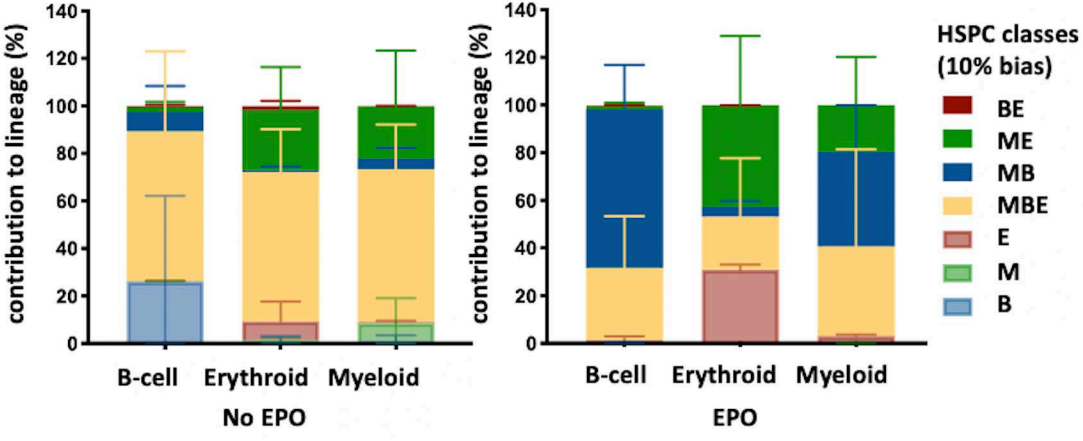
contribution to lineage (%)
140
120
100
80
60
40
20
0
B-cell
Erythroid
Myeloid
No EPO
EPO
HSPC classes
(10% bias)
BE
ME
MB
MBE
E
M
B

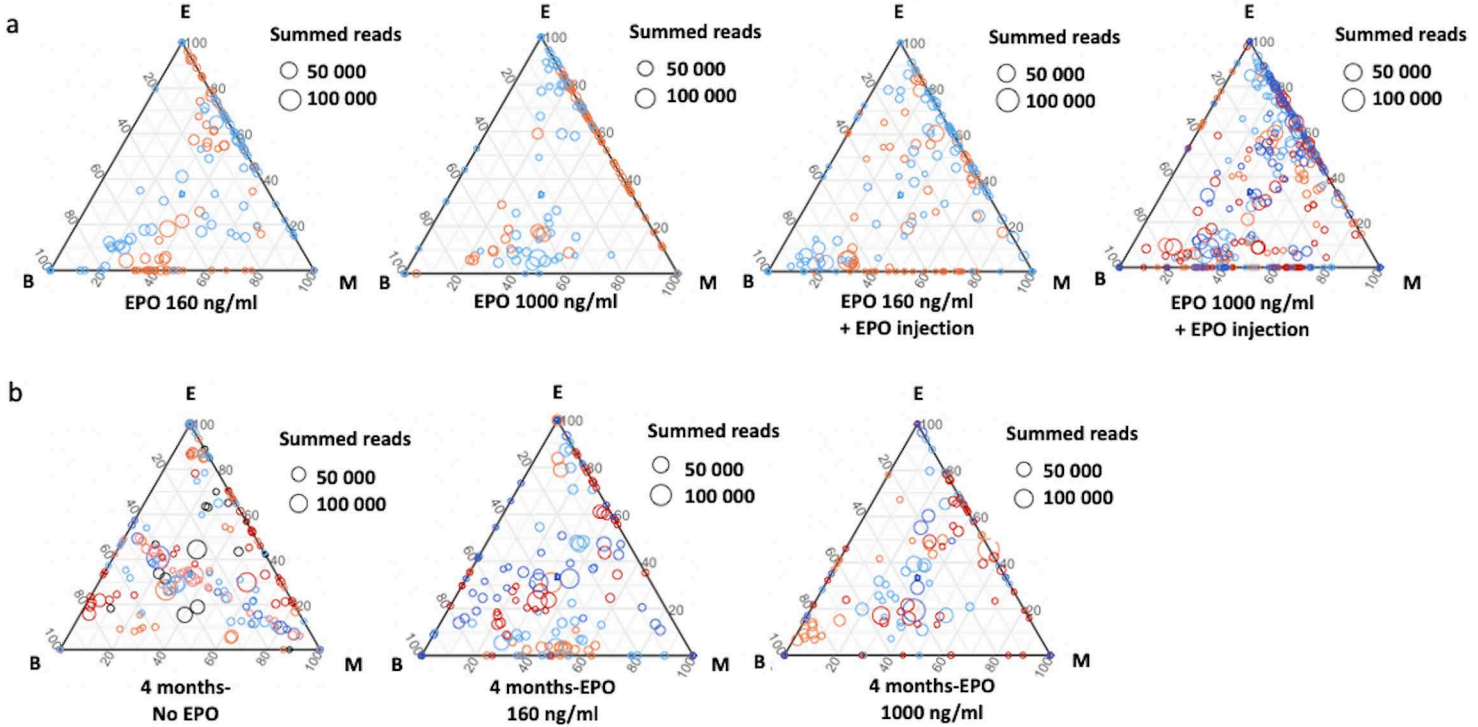
a
E
B
M
Summed reads
50 000
100 000
EPO 160 ng/ml
EPO 1000 ng/ml
EPO 160 ng/ml
+ EPO injection
EPO 1000 ng/ml
+ EPO injection
b
4 months-
No EPO
4 months-EPO
160 ng/ml
4 months-EPO
1000 ng/ml

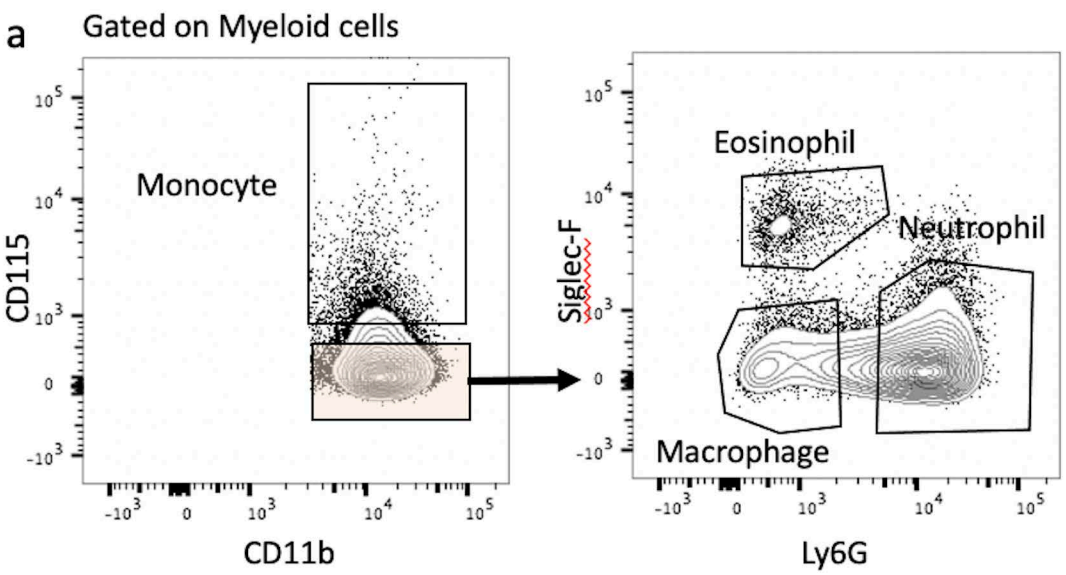
a
Gated on Myeloid cells
Monocyte
CD115
CD11b
Eosinophil
Neutrophil
Macrophage
Siglec-F
Ly6G

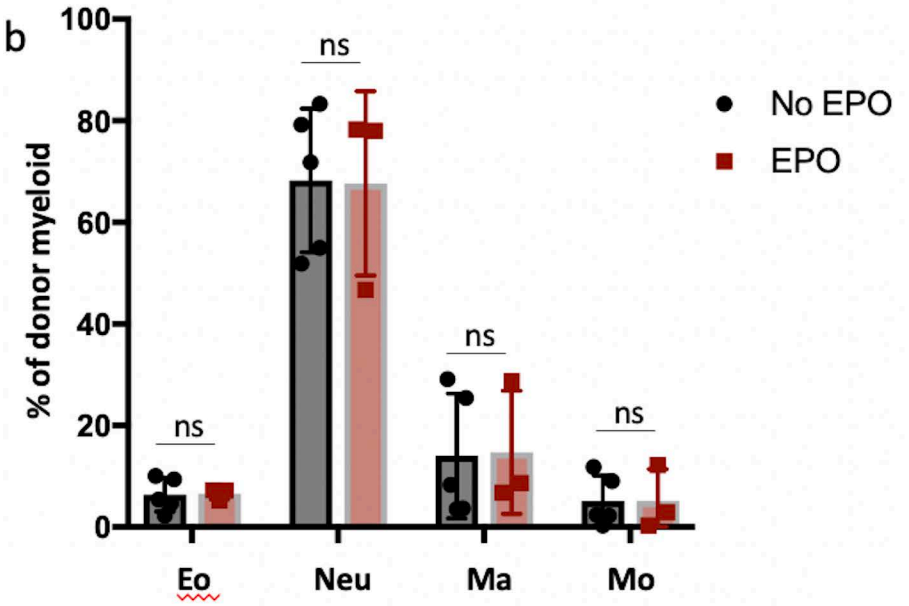
b
% of donor myeloid
ns
ns
ns
ns
No EPO
EPO
Eo
Neu
Ma
Mo

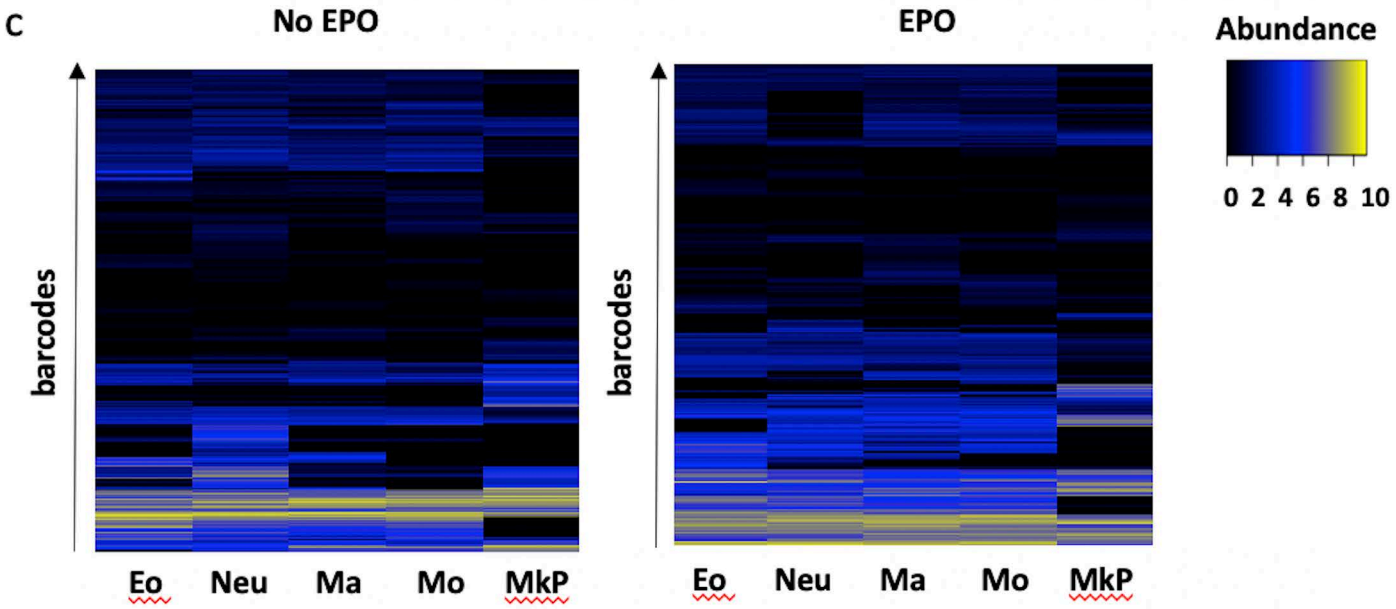
c
No EPO
EPO
Abundance
0 2 4 6 8 10
barcodes
Eo
Neu
Ma
Mo
MkP

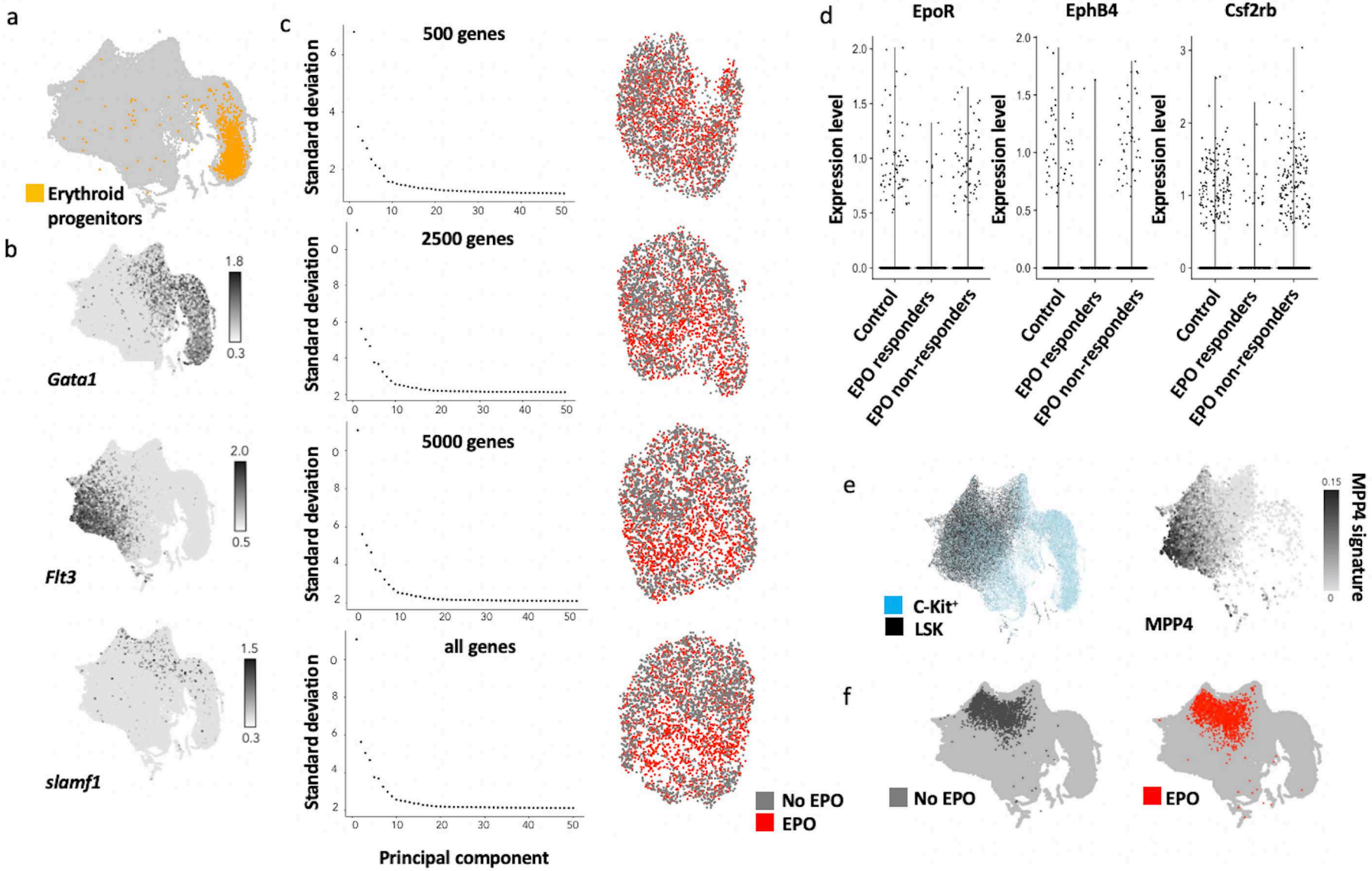
a
Erythroid progenitors
b
Gata1
1.8
0.3
Flt3
2.0
0.5
slamf1
1.5
0.3
c
500 genes
2500 genes
5000 genes
all genes
Standard deviation
Principal component
No EPO
EPO
d
EpoR
EphB4
Csf2rb
Expression level
Control
EPO responders
EPO non-responders
e
C-Kit+
LSK
MPP4
MPP4 signature
0.15
0
f
No EPO
EPO

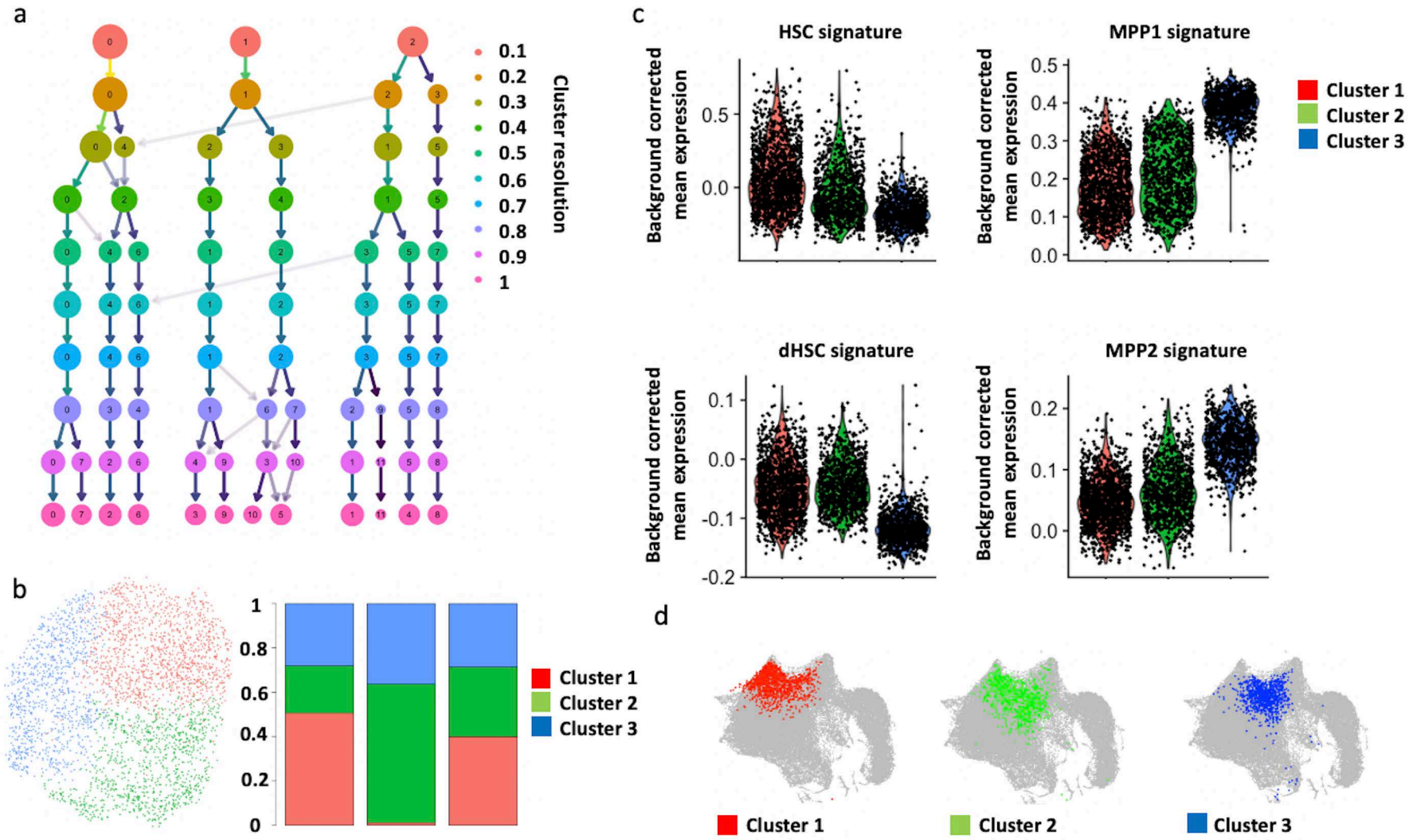
a
0.1
0.2
0.3
0.4
0.5
0.6
0.7
0.8
0.9
1
Cluster resolution
b
Cluster 1
Cluster 2
Cluster 3
c
HSC signature
MPP1 signature
dHSC signature
MPP2 signature
Background corrected mean expression
Cluster 1
Cluster 2
Cluster 3
d
Cluster 1
Cluster 2
Cluster 3

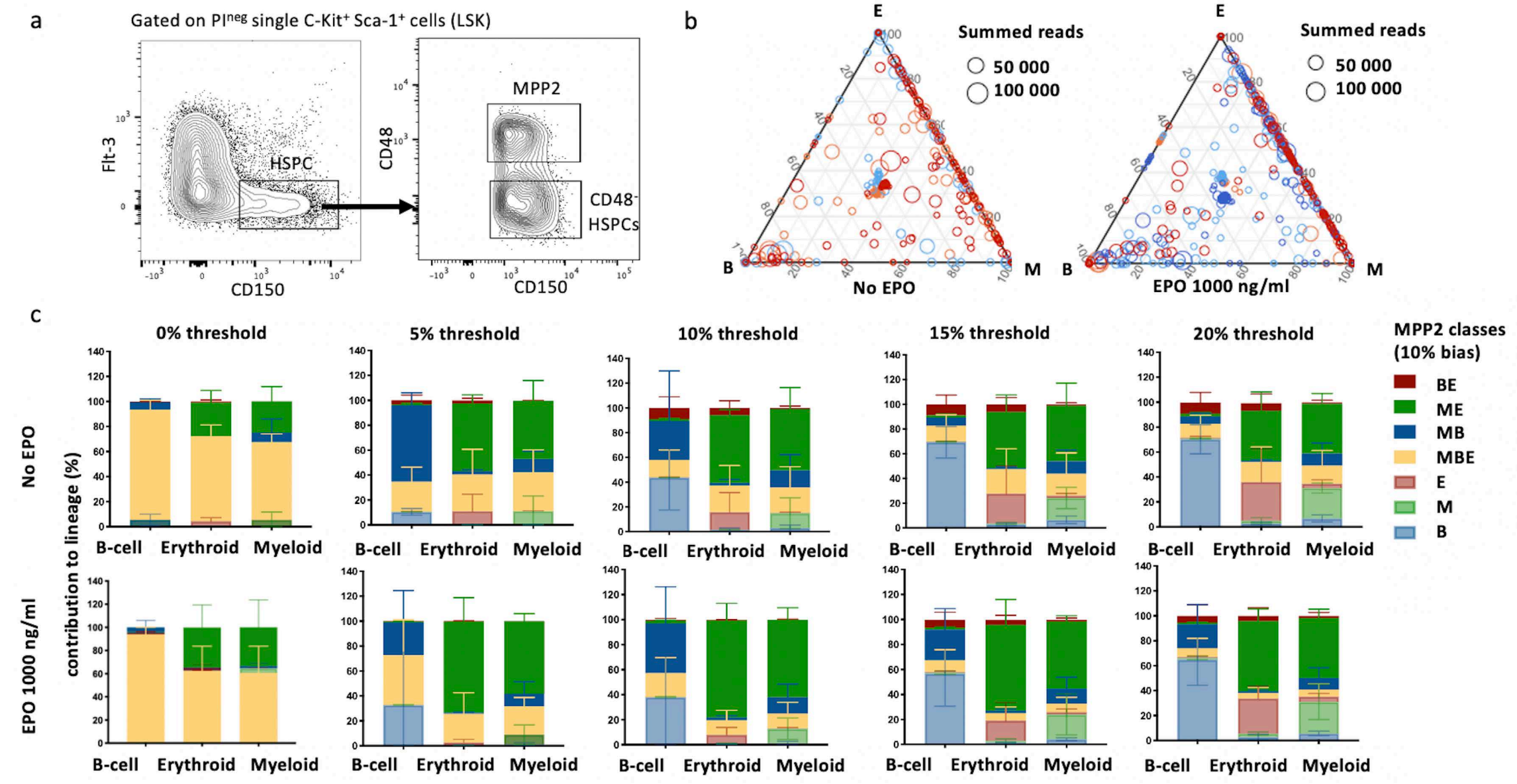
a
Gated on PI^neg single C-Kit+ Sca-1+ cells (LSK)
Flt-3
HSPC
CD150
CD48
MPP2
CD48-
HSPCs
CD150
b
E
Summed reads
50 000
100 000
B
M
No EPO
EPO 1000 ng/ml
c
0% threshold
5% threshold
10% threshold
15% threshold
20% threshold
MPP2 classes
(10% bias)
BE
ME
MB
MBE
E
M
B
No EPO
EPO 1000 ng/ml
contribution to lineage (%)
B-cell
Erythroid
Myeloid

Supplementary File 1: Permutation testing of changes in clonality after transplantation of EPO-exposed HSPCs. Same data as in Figure 1 figure supplement 4 and Figure 1 figure supplement 3. HSPCs were cultured with EPO (1,000 ng/ml) for 16h. Barcodes in the erythroid (E), myeloid (M), B-lymphoid (B) lineage, dendritic cell (DC) and HSPCs, were analyzed four weeks after transplantation and categorized by bias using a 10% threshold. The output of MB and ME classified barcodes to the B, M, and E lineages was analyzed using a permutation test. By permutating the mice of control and EPO groups, the random distribution of this output was generated and compared to the real output difference between control and EPO group. A p-value was generated using permutation testing.

Figure 1 figure supplement	**Condition**	**p-value**			
		MB in B	**MB in M**	**ME in E**	**ME in M**
3	**HSPCs 1000 ng/ml repeat**	0.01	0.0083	0.0087	0.0087
4	**HSPCs 1000 ng/ml - 6 weeks timepoint**	0.01	0.01	0.0138	0.0185